Petroleum Science 22 (2025) 5296–5313

Contents lists available at ScienceDirect

Petroleum Science

journal homepage: www.keaipublishing.com/en/journals/petroleum-science

Original Paper

A new approach to remediation of crude oil with promising green composites: Biosurfactant-producing *Bacillus* sp. consortium entrapped in chitosan, chitosan/glutaraldehyde and chitosan/Na-bentonite

Sezen Bilen Ozyurek *, Kaan Soyuer, Arda Ustundag

Department of Biology (Biotechnology), Faculty of Science, Hacettepe University, Ankara, Beytepe, 06800, Türkiye

ARTICLE INFO

Article history:
Received 22 October 2024
Received in revised form
4 July 2025
Accepted 24 September 2025
Available online 29 September 2025

Edited by Min Li

Keywords:
Chitosan
Glutaraldehyde
Na-bentonite
Immobilization
Entrapped bacterial consortium
Crude oil removal
Biosurfactant
Ex-situ simulation study

ABSTRACT

This study compares the crude oil removal efficiency of free and biosurfactant-producing bacterial consortia (*Bacillus tequilensis* NR_104919 and *Bacillus axarquiensis* NR_115929) entrapped in chitosan (CH), chitosan/glutaraldehyde (CH/GA), and chitosan/Na-bentonite (CH/BNT) matrices. Additionally, the mechanical and thermal stability, swelling capacity, surface morphology, and chemical bonding of these composites were evaluated. Initially, the biosurfactant produced by the consortium was identified using screening methods, and its lipopeptide structure was confirmed through TLC and ^{1}H NMR analyses, with a yield of 0.2 g/L. Following characterization, the biosurfactant-producing bacterial consortium was immobilized onto CH, CH/GA, and CH/BNT beads for further assessment. When comparing the oil removal capacities of the composites, the consortium immobilized in the CH/BNT matrix exhibited significantly higher crude oil removal efficiency than those entrapped in CH, CH/GA, and the free consortium. The maximum oil removal by the CH/BNT-entrapped consortium was achieved under optimized conditions: 0.5 mL crude oil, 0.1 g Na-bentonite, pH = 6.0, at 35 °C, over a 7-day incubation period. However, a decline in oil remediation performance was observed from the fourth reuse cycle onward. These laboratory-scale findings were further validated through ex-situ simulation and long-term experiments, confirming the potential of the CH/BNT composite for effective and sustainable petroleum pollutant remediation. The swelling capacity of inactivated CH was comparable to that of the CH/BNT composite, with both exhibiting greater swelling than CH/GA beads. Additionally, CH/BNT beads demonstrated superior mechanical stability relative to CH and CH/GA, which showed similar stability profiles. Thermal stability, surface morphology, and chemical bonding of the CH, CH/GA, and CH/BNT composites were characterized using TGA, FT-IR, and SEM analyses. CH/BNT composite represents an effective, economical, and environmentally benign alternative to costly synthetic materials for the remediation of oil pollution in aquatic environments. This study highlights the potential of chitosan/Na-bentonite-based composites as sustainable solutions for petroleum pollutant removal, while recommending pilot-scale investigations to assess their feasibility and performance under real-world conditions.

1. Introduction

The accelerating pace of industrial, agricultural, and municipal development, coupled with unprecedented global population growth, has significantly elevated the global demand for petroleum, which is projected to reach 100.90 million barrels per day. This growing demand has intensified petroleum industry operations, including exploration, transportation, and processing activities, which are frequently associated with oil spills caused by

* Corresponding author.
E-mail address: sbilen@hacettepe.edu.tr (S.B. Ozyurek).
Peer review under the responsibility of China University of Petroleum (Beijing).

https://doi.org/10.1016/j.petsci.2025.09.039

pipeline ruptures, refinery discharges, and improper storage or handling of petroleum derivatives. These incidents constitute major sources of petroleum hydrocarbon pollution, posing severe risks to both marine and terrestrial ecosystems as well as to human health. Once released into the environment, spilled oil undergoes complex physical and chemical transformations that result in contamination of water sources and the development of unpleasant tastes and odors in drinking water. Moreover, increasing oil pollution from sectors such as food processing, catering, and crude oil extraction has emerged as an environmental concern, highlighting the urgent need for sustainable pollution management and remediation strategies (Chettri et al., 2021; Eweida et al., 2023; Khandelwal et al., 2022; Luo et al., 2021; Mekonnen et al., 2024; Singha and Pandey, 2021). Traditional mechanical, physical, and chemical remediation methods are often neither cost-effective nor environmentally sustainable. Moreover, these approaches can produce harmful by-products that pose risks to public health and the environment (Khandelwal et al., 2022; Mekonnen et al., 2024; Singha and Pandey, 2021). In contrast, bioremediation has gained recognition as an effective, eco-friendly, sustainable, and cost-efficient approach. It enables the biological conversion, disintegration, detoxification, or transformation of harmful organic contaminants, including industrial effluents, heavy metals, xenobiotic compounds, organic halogens, pesticides, and chlorinated compounds in wastewater and soil environments (Aragaw, 2021; Kuppan et al., 2024; Mekonnen et al., 2024; Sayara and Sánchez, 2020; Sharma, 2020). Various microorganisms, including bacteria, fungi, and some algae, as well as plants or their metabolites like enzymes, can completely mineralize environmental pollutants into carbon dioxide, water, inorganic compounds, cell proteins, and simple organic molecules (Ali et al., 2020; Das and Chandran, 2011; Huang et al., 2019; Jabbar et al., 2022; Khandelwal et al., 2022; Luo et al., 2021; Mekonnen et al., 2024; Parach et al., 2017; Safdari et al., 2017; Spini et al., 2018; Sohail and Jamil, 2019). However, individual bacterial strains often face challenges such as competition with native microbes, antibiotic pressures, environmental fluctuations, and predation, which limit their bioremediation potential (Juhanson et al., 2009; Khandelwal et al., 2022; Siles and García-Sánchez, 2018). To overcome these limitations, bacterial consortia composed of diverse strains with complementary metabolic pathways offer greater robustness and stability, thereby enhancing crude oil degradation under variable conditions (Hazaimeh et al., 2014). However, the biological activity of microorganisms is significantly influenced by various environmental factors, including energy sources, bioavailability, oxygen and nutrient availability, pH, temperature, crude oil characteristics, and soil type; all of which play critical roles in determining the success of petroleum hydrocarbon remediation (Mekonnen et al., 2024). One of the main challenges limiting the effectiveness of biodegradation, particularly in the context of crude oil remediation, is the inherent low aqueous solubility, non-polarity, and hydrophobic nature of crude oil. These physicochemical properties restrict the bioavailability of hydrocarbons to microorganisms, thereby impeding their degradation. To address this limitation, the use of non-toxic surfactants is essential as they enhance the solubility and bioavailability of crude oil components (Khandelwal et al., 2022; Partovinia and Rasekh, 2018). Surfactants are classified into two main groups: (i) chemical surfactants originating from petrochemical or oleochemical sources, and (ii) biosurfactants, which are heterogeneous amphiphilic compounds synthesized either as part of the microbial cell membrane or secreted extracellularly by microorganisms. Among these, biosurfactants are considered more effective and cost-effective than their chemical counterparts, primarily due to their low critical micelle concentration (CMC). Additionally, biosurfactants offer significant advantages, including environmental compatibility, biodegradability, low toxicity, ecological safety, cell specificity, high activity, and relative ease of synthesis and extraction (Batool et al., 2017; Jabbar et al., 2022; Sohail and Jamil, 2019). Biosurfactant facilitates the bioremediation effectiveness of microbial strains through the following mechanism: (i) increasing the bioavailability hydrophobic substrate for microbial strains, (ii) facilitating the adhesion and de-adhesion of bacterial strains to hydrophobic substrates, (iii) promoting micellization, leading to pollutant desorption (Gaur et al., 2021; Jabbar et al., 2022). Biosurfactants have multifunctional applications in the petroleum and gas industries, including cleaning up oil spills, removing sludge from petroleum tanks, and improving petroleum quality. In addition to oily sludge treatment and oil spill remediation, they also show significant potential for remediating heavy metal pollution, pesticide contamination, and cleaning oil reservoirs. Although biosurfactants are a promising alternative to chemical surfactants in bioremediation within the petroleum industry, they may be less effective at high pollutant concentrations (De Almeida et al., 2016; Eraqi et al., 2016; Gaur et al., 2021; Sohail and Jamil, 2019). Therefore, future research should prioritize the development of cost-effective biosurfactant production methods that not only achieve higher yields but also mitigate the detrimental impacts of environmental fluctuations. One promising strategy to enhance both the stability and productivity of biosurfactant-producing microorganisms is microbial immobilization (Thio et al., 2022).

The immobilization of microbial cells offers protection against extreme environmental conditions and toxic compounds, enhances cellular stability, and mitigates risks associated with contamination. This process shields microorganisms from environmental stresses, toxicity from co-contaminants, competition with native microbial populations, and predation, thereby improving their survival and overall bioremediation efficiency (Berillo et al., 2021; Mehrotra et al., 2021; Mekonnen et al., 2024; Partovinia and Rasekh, 2018; Siles and García-Sánchez, 2018). Additionally, immobilization reduces labor costs and facilitates the reuse of microbial cells, rendering the bioremediation process more economical (Wahba, 2017). Common immobilization techniques include the entrapment and encapsulation of microorganisms within polymeric matrices, as well as their attachment to solid supports (Berillo et al., 2021; Partovinia and Rasekh, 2018). In the context of oil spill remediation, sorbent materials have emerged as effective agents due to their cost-efficiency and minimal environmental impact (Eweida et al., 2023). Ideal sorbents exhibit properties such as high hydrophobicity and oleophilicity, rapid sorption rates, substantial uptake capacity, low water retention, insolubility, buoyancy, and affordability. Both natural polymers including dextran, agar, agarose, alginate, chitosan, collagen, seaweed, dead mushroom biomass, rice hulls, and lignin and synthetic polymers such as polyacrylamide, polyvinyl alcohol, polyethylene glycol, polycarbamoyl sulfonate, polypropylene, polyethylene, polyvinyl chloride, polyurethane, and polyacrylonitrile are widely employed to fabricate carriers that are inexpensive, non-toxic, and possess reactive functional groups (Berillo et al., 2021; Eweida et al., 2023; Khandelwal et al., 2022; Mehrotra et al., 2021; Partovinia and Rasekh, 2018). Natural carriers are preferred for bacterial cell immobilization due to their non-toxic and eco-friendly nature consequently, natural adsorbents such as bentonite, lignin, chitosan, and biochar have garnered significant research interest in recent years (Hazaimeh et al., 2014; Zhu et al., 2023).

Chitosan, a linear polycationic heteropolysaccharide biopolymer composed of glucosamine and N-acetylglucosamine residues linked by β-(1→4) glycosidic bonds, is easily obtained

through the deacetylation of chitin (Eweida et al., 2023). It exhibits favorable physical and biological properties for microorganism accumulation, including biocompatibility, non-toxicity, low immunogenicity, biodegradability, and ease of chemical modification, rendering it an ideal biopolymer for microbial immobilization (Khondee et al., 2015; Luo et al., 2021; Zhu et al., 2023). Nonetheless, chitosan exhibits certain limitations that constrain its practical use as an adsorbent, such as a relatively low surface area, high solubility in acidic environments, and chemical instability. Furthermore, chitosan beads often exhibit mechanical weakness due to their inherently soft structure, making them susceptible to fragmentation under mechanical stress, particularly in large-scale applications, which limits their practical utility (Wahba, 2017; Yang et al., 2024). To overcome these challenges, chitosan beads can be chemically activated using crosslinking agents such as glutaraldehyde or combined with materials like Na-bentonite to enhance their properties (Cengiz et al., 2012; Kaushal et al., 2018). Specifically, immobilizing bentonite onto a carrier with suitable size and sorption capacity improves both the mechanical stability of the composite beads and their oil removal efficiency, thereby overcoming key limitations associated with chitosan-based adsorbents (Wang et al., 2019). Clay minerals have been extensively utilized across various applications due to their high cation exchange capacity, swelling ability, large specific surface area, and consequently strong adsorption properties (Xi et al., 2010). Bentonite, primarily composed of montmorillonite, is a natural porous clay mineral characterized by a crystal structure consisting of an aluminum octahedral layer sandwiched between two silica tetrahedral layers. Its flaky morphology, moderate cation exchange capacity, and reactive hydroxyl groups on the surface contribute to its widespread use, particularly in the bleaching of edible and mineral oils. Owing to its abundance and low cost, bentonite finds applications in diverse sectors such as mineral oil refining, paints, cosmetics, and pharmaceuticals (Abulimiti et al., 2023; Belousov et al., 2021; Chen et al., 2020; Khodabakhshloo et al., 2021). Additionally, bentonite serves as a binder, adsorbent especially in drilling mud and filler (Abulimiti et al., 2023; Alexander et al., 2019; Dotto et al., 2021; Kim et al., 2020). Recent studies have highlighted sodium bentonite's strong adsorption capacity for toxic metals and dyes, attributed to its high cation exchange capacity and large specific surface area. Moreover, these natural materials are increasingly investigated to mitigate environmental pollution caused by oil spills and for the recovery of valuable natural resources. Recent research has focused on integrating clay minerals into natural polymer matrices to enhance adsorption performance, aiming particularly at high-efficiency remediation applications. Polymer–clay composite materials have garnered significant attention due to their enhanced mechanical strength, improved thermal stability, increased flame resistance, and superior capacity for removing crude oil, heavy metals, and textile dyes from wastewater (Ferhat et al., 2016; Mokhtar et al., 2024; Santoso et al., 2019; Wang et al., 2019).

The current study aims to: (1) Screen environmental strains of *Bacillus tequilensis* and *Bacillus axarquiensis* for biosurfactant production; (2) Extract, purify, and characterize biosurfactants via acid precipitation, Thin Layer Chromatography (TLC), and ^{1}H Nuclear Magnetic Resonance (^{1}H NMR); (3) Prepare chitosan, chitosan/glutaraldehyde, and chitosan/sodium bentonite composites entrapping a consortium of potent biosurfactant-producing *Bacillus* spp.; (4) Compare crude oil removal efficiencies among the entrapped composites; (5) Optimize growth conditions to maximize oil removal efficacy; (6) Assess reusability of the most effective entrapped composite; (7) Conduct simulation studies for ex-situ petroleum removal and evaluate composite sustainability during long-term application; (8) Compare swelling capacities, mechanical stabilities, and surface zero-point charges of the entrapped beads; (9) Characterize entrapped composites using Thermogravimetric Analysis (TGA), Fourier Transform Infrared Spectroscopy (FT-IR), Scanning Electron Microscopy (SEM), and to identify and thermal stabilities, chemical composition, functional groups, bond types, structural morphologies; (10) Perform statistical analysis of all experimental results.

2. Materials and methods

2.1. Chemicals

Glucose (ISOLAB, Germany), yeast extract, Nutrient Broth (NB) (Condalab, Spain), Bushnell Hass Broth (BHB) (HiMedia, India, #M350), NaOH, dichloromethane, chloroform, methanol, deuterated dimethylsulfoxide (d6-DMSO), Triton X-100, glycerol, TLC, glacial acetic acid (100%) (Merck, Germany), hydrochloric acid (37%) (HCl) (Isolab, Germany), Brain-Heart Infusion Broth (BHI), (Sigma-Aldrich, USA), glutaraldehyde (25% in H_2O) (Sigma-Aldrich, Germany), chitosan, anthron, iodine, ninhydrin (CDH, India), crude oil (API gravity = 45.37, specific gravity 0.800, density of the fluid/density of water) were obtained from an oil field in Diyarbakır, Türkiye. Sodium-bentonite (Na-BNT) obtained from Samaş Mine in Reşadiye, Tekirdağ, Türkiye. The clay mineral, which complies with API 13A (non-treated bentonite) standards, is sodium-rich and contains at least 90% montmorillonite, with the following chemical composition: SiO_2 (61.28%), Al_2O_3 (17.79%), Fe_2O_3 (3.01%), CaO (4.54%), Na_2O (2.70%), MgO (2.10%), K_2O (1.24%).

2.2. Microorganisms

In this study, the environmental-origin strains *Bacillus tequilensis* NR_104919 and *Bacillus axarquiensis* NR_115929 were utilized. These strains were preserved in BHI medium supplemented with 10% glycerol at the Hacettepe University Culture Collection Laboratory (Bilen Ozyurek and Seyis Bilkay, 2017).

2.2.1. Preparation of individual bacterial strains

Pure cultures of each bacterial strain were inoculated into nutrient broth (NB) medium supplemented with 1% glucose and incubated at 30 °C for 24 h with shaking at 150 rpm (Miprolab, Türkiye). Then, the individual bacterial strain was then centrifuged at 4650 × *g* for 10 min (NF 1200, Nuve, Türkiye) and the resulting cell pellets were suspended in sterile 0.9% (*w*/*v*) NaCl solution at pH = 7.0, and the optical density at 600 nm was adjusted to 1.0 using a UV spectrophotometer (Shimadzu-UV1700, Japan) (Khondee et al., 2015). The presence of biosurfactants was assessed using bacterial cultures standardized to equivalent growth densities.

2.2.2. Preparation bacterial consortium

The potent bacterial strains were cultured in NB medium at 30 °C with agitation at 150 rpm for approximately 18 h. Following adjustment of the bacterial cultures to equivalent growth densities, the inocula were combined in a 1:1 ratio to establish a bacterial consortium (Costa et al., 2014).

2.3. Biosurfactant production with bacterial consortium

A 100 mL BHB medium was prepared in a 250 mL Erlenmeyer flask with the following composition: 0.2 g/L $MgSO_4$, 0.02 g/L $CaCl_2$,1.0 g/L KH_2PO_4, 1.0 g/L K_2HPO_4, 1.0 g/L NH_4NO_3, 0.05 g/L $FeCl_3$ supplemented with 1% (*v*/*v*) glucose as the carbon source, 1% (*w*/*v*) yeast extract as the nitrogen source, and 0.1% (*v*/*v*) trace element solution containing (mg/L): 0.08 mg/L $FeCl_3{\cdot}6H_2O$, 0.75 mg/L

$ZnSO_4{\cdot}7H_2O$, 0.75 mg/L $MnSO_4{\cdot}H_2O$, 0.075 mg/L $CuSO_4{\cdot}5H_2O$, 0.08 mg/L $CoCl_2{\cdot}6H_2O$. The BHB medium was adjusted to pH = 7.0 using 1 M NaOH. 1% (*v*/*v*) bacterial consortium was inoculated into 100 mL of sterile BHB medium, and the culture was incubated at 30 °C with shaking at 150 rpm for 7 days (Miprolab, Türkiye) (Soyuer and Bilen Ozyurek, 2024).

2.4. Screening methods for detecting biosurfactant production

Following the incubation period, the entire culture broth was sequentially centrifuged at 4650 × *g* for 10 min using an NF 1200 centrifuge (Nuve, Türkiye) and at 10752 × *g* for 10 min using an Eppendorf 5417C centrifuge (Germany). The supernatants subsequently were filtered through a 0.45 μm pore size cellulose acetate (CA) syringe filter (Millipore, Sartorius, USA). The resulting cell-free culture supernatants were transferred to clean test tubes. Triton X-100 and distilled water were employed as the positive and negative controls, respectively.

2.4.1. Drop-collapse assay

The drop-collapse assay was performed using 96-well microplates, each well pre-coated with 5 μL of mineral oil (Sigma-Aldrich; density = 0.84 g/mL at 25 °C). Subsequently, 5 μL of cell-free culture supernatant—obtained from cultures incubated at 30 °C with shaking at 150 rpm for 7 days—was gently applied to the oil-coated wells. After 1 min, the droplet morphology was observed. Collapse or spreading of the droplet was interpreted as a positive indication of biosurfactant production. This assay was performed and evaluated in accordance with protocols established in previous studies (Gaur et al., 2021; Ghazi Faisal et al., 2023; Jain et al., 1991).

2.4.2. Oil displacement assay

The oil displacement assay was conducted to detect the presence of biosurfactants using a small volume of the sample. Approximately 30 mL of distilled water was added to a 90 mm diameter Petri dish, followed by the addition of 20 μL of oil to form a thin oily layer on the water surface. Subsequently, 50 μL of cell-free culture supernatant was carefully applied onto the oil-covered surface. After 30 s, the diameter of the spreading area was measured (Gaur et al., 2021; Ghazi Faisal et al., 2023; Morikawa et al., 2000).

2.4.3. Emulsification activity (E_{24})

To assess the emulsification activity, 2 mL of cell-free culture supernatant was mixed with an equal volume (2 mL) of mineral oil. The mixture was vigorously vortexed at maximum speed for 3 min and then allowed to stand at room temperature for 24 h before measurement. E_{24} was calculated using Eq. (1) (Goveas et al., 2022; Sohail and Jamil, 2019).

$$E_{24}\ (\%) = \frac{\text{Height of the emulsified layer}}{\text{Total height of the liquid layer}} \times 100\% \quad (1)$$

2.5. Extraction, purification and characterization of biosurfactant

The biosurfactant was extracted using a combination of acid precipitation and solvent extraction, following the method described by Eraqi et al. (2016) and Soyuer and Bilen Ozyurek (2024). The pH of the cell-free culture supernatant was adjusted to 2.0 using 6 N HCl. The acidified supernatant was refrigerated at 4 °C overnight. After refrigeration, the supernatant was centrifuged at 4650 × *g* for 10 min using a NF 1200 centrifuge. An equal volume of chloroform: methanol (2:1, *v*/*v*) was added to the supernatant at room temperature. The mixture was agitated at 150 rpm for 10 min and allowed to stand until phase separation occurred. The formation of a grey or white-colored precipitate indicated the presence of biosurfactants. During the solvent extraction, three distinct phases were observed: (1) organic phase, (2) emulsified phase, and (3) aqueous phase. The emulsified layer, which contained the biosurfactant, was carefully collected and transferred to a glass Petri dish. The solvents were evaporated in a fume hood at room temperature for 24 h to obtain the biosurfactant (Hedlab, Türkiye). A dark brown oily precipitate was recovered as the partially purified biosurfactant. The biosurfactant was quantified gravimetrically by measuring its dry weight (g/L). The recovered biosurfactant was stored at 4 °C for short-term use and at −20 °C for long-term preservation (Gaur et al., 2021; Ghazi Faisal et al., 2023; Ibrahim, 2018; Kumar et al., 2016; Sohail and Jamil, 2019).

Thin Layer Chromatography (TLC) was carried out to purify the biosurfactant. A sample of 0.1 g of extracted biosurfactant was dissolved in a solvent mixture of methanol: chloroform (95:5, *v*/*v*) at room temperature. The dissolved sample was then carefully spotted onto a silica gel plate, with the baseline positioned approximately 1 cm from the bottom of the plate. After drying, the TLC plate was placed in a development tank containing the mobile phase, a mixture of chloroform: methanol: water (65:25:4, *v*/*v*) (mobile phase). The plate was allowed to develop until the solvent front reached an appropriate height. TLC plate visualized under UV-spectrophotometer using arthron (*w*/*v*) (1%), iodine (*w*/*v*) (3%), and ninhydrin (*w*/*v*) (0.25%) reagents to detect the presence of sugar, lipid, and amino groups, respectively (Balan et al., 2016; Batool et al., 2017; Singh et al., 2019; Thio et al., 2022). The retardation factor (R_f) values of the moiety of peptide, lipid and carbohydrate spots on the TLC plate were calculated as the distance traveled by the solute over the distance traveled by the solvent (cm) (Sun et al., 2018; Chaurasia et al., 2020). ^{1}H NMR analysis of the purified biosurfactant was performed with Bruker 400 MHz AV NMR spectrometer (Germany) using deuterated DMSO as the solvent (Soyuer and Bilen Ozyurek, 2024).

2.6. Preparation of chitosan, chitosan/glutaraldehyde, and chitosan/bentonite beads entrapped with biosurfactant-producing consortia

2.6.1. Entrapment of bacterial consortia into chitosan and chitosan/bentonite beads

To prepare the chitosan solution, 2.5 g of chitosan was dissolved in 45 mL of 5% sterile glacial acetic acid by stirring until fully dissolved. Subsequently, 0.2 g of bentonite was added, and the mixture was magnetically stirred at 400 rpm (IKA, Germany) for 1 h to achieve a uniform solution, which was then stored at 4 °C for 18 h. Following this, 5 mL of the prepared bacterial consortium (1:1 *v*/*v*) was separately added to 45 mL of both 3% (w/v) chitosan and chitosan/bentonite solutions. The mixtures were stirred at 150 rpm for 5 min and allowed to stand at room temperature for 10 min. Beads were formed by dropping the solution into a 1 M NaOH solution containing 26% ethanol (*v*/*v*), yielding approximately 45 g of chitosan and chitosan/bentonite beads. These beads were gently stirred at 400 rpm for 1 h at room temperature, then removed, washed three times with 200 mL of sterile distilled water, and stored in cold phosphate buffer (pH = 7.0) for 24 h (Costa et al., 2014; Gur et al., 2018; Purnomo et al., 2023; Wang et al., 2019).

2.6.2. Activation of the chitosan beads with glutaraldehyde

To prepare the cross-linking solution, 10 g of CH beads were treated with 15 mL of a 2.5% glutaraldehyde solution (prepared by mixing 15 mL of glutaraldehyde with 85 mL of distilled water). The activation process was carried out with stirring at room temperature for 3 h (Biosan, Latvia). After activation, the CH/GA beads were collected using a sieve and washed three times with sterile distilled water to remove any unreacted glutaraldehyde (Gur et al., 2018).

2.7. Crude oil removal with entrapped-CH, CH/GA and CH/BNT beads

A 50 mL Bushnell Hass Broth (BHB) medium was prepared in a 250 mL Erlenmeyer flask containing 1% Triton X-100 (*v*/*v*), 1% yeast extract (*w*/*v*), 0.1% glucose (*w*/*v*), and 0.1% trace elements (*v*/*v*), supplemented with 1% crude oil (g/L). The medium was sterilized using a cellulose acetate (CA) syringe filter with a 0.45 μm pore size (Millipore, USA). Then, 1 mL of free bacterial consortia and 10 g of entrapped CH, CH/GA, and CH/BNT beads were inoculated into fresh BHB medium (pH = 7.0). Incubation was carried out at 30 °C with shaking at 125 rpm for 7 days (Miprolab, Türkiye). Experiments were performed in triplicate, including both biotic and abiotic controls. Oil residues were measured gravimetrically, and the removal efficiencies of the free and entrapped consortia were compared (Bilen Ozyurek and Seyis Bilkay, 2020; Farid et al., 2024).

2.7.1. Optimization of the main factors affecting crude oil removal with potent entrapped bead

Several parameters were optimized to achieve the highest petroleum removal efficiency using the potent composite, including Na-bentonite amount (0.025, 0.05, 0.1, 0.2, 0.4 g), crude oil concentration (0.25, 0.5, 0.75, 1 g/50 mL), incubation temperature (20, 25, 30, 35, 40 °C), initial pH (5.0, 6.0, 7.0, 8.0, 9.0), salinity (0, 2.5, 5, 7.5, 10%), and incubation period (1, 3, 5, 7, 9 days) (Chen et al., 2017). Petroleum removal efficiency was determined by gravimetric analysis.

2.7.1.1. Effect of varying Na-bentonite amount on crude oil removal. 10 g of CH/BNT beads, prepared with different amounts of Na-bentonite (0.025, 0.05, 0.1, 0.2, and 0.4 g), were inoculated into BHB medium (pH = 7.0) supplemented with 1% crude oil (g/L). Incubation was performed at 30 °C with shaking at 125 rpm for 7 days.

2.7.1.2. Effect of crude oil concentration on removal. 10 g of CH/BNT beads, exhibiting the highest removal efficiency, were inoculated into BHB medium supplemented with crude oil at concentrations of 0.25, 0.5, 0.75, and 1 g/50 mL. Incubation was performed at 30 °C with shaking at 125 rpm for 7 days.

2.7.1.3. Effect of incubation temperature on crude oil removal. 10 g of CH/BNT beads were inoculated into BHB medium supplemented with optimal oil concentration. The incubation was performed at varying temperatures (20, 25, 30, 35, and 40 °C) with shaking at 125 rpm for 7 days.

2.7.1.4. Effect of initial pH on crude oil removal. 10 g of CH/BNT beads were inoculated into BHB medium prepared at different pH values (5.0, 6.0, 7.0, 8.0, and 9.0) and supplemented with the optimal oil concentration. Incubation was conducted at the optimal temperature with shaking at 125 rpm for 7 days.

2.7.1.5. Effect of salinity on crude oil removal. 10 g of CH/BNT beads were inoculated into BHB medium prepared at the optimal pH, supplemented with the optimal oil concentration, and adjusted to varying salt concentrations (0%, 2.5%, 5%, 7.5%, and 10%). Incubation was carried out under optimal temperature conditions with shaking at 125 rpm for 7 days.

2.7.1.6. Effect of incubation period on crude oil removal. 10 g of CH/BNT beads were inoculated into BHB medium prepared at the optimal pH, supplemented with optimal oil and salt concentrations. Incubation was performed under optimal temperature conditions with shaking at 125 rpm for 1, 3, 5, 7, and 9 days.

2.7.2. Reusability

The entrapped potent composite was added to fresh BHB medium, and incubation was carried out under optimized conditions. The reusability of the potent carrier material for petroleum removal was evaluated (Kaushal et al., 2018).

2.7.3. Crude oil removal

The residual crude oil was extracted with an equal volume (1:1, *v*/*v*) of dichloromethane (CH_2Cl_2). The residual crude oil was quantified gravimetrically after evaporating the solvent at 95 °C for 30 min. The percentage of the removal was calculated using Eq. (2) (Gaur et al., 2021; Patowary et al., 2017).

$$\text{Removal } (\%) = \frac{(p_0 - p_1 - p_2)}{p_0} \times 100\% \quad (2)$$

The degradation data was calculated using Eqs. (3) and (4) (Khandelwal et al., 2022).

$$kt = \ln\left(\frac{c_o}{c_t}\right) \quad (3)$$

$$t_{\frac{1}{2}} = \frac{0.693}{k} \quad (4)$$

c_o and c_t show the initial and final concentrations of crude oil, g/L, k is degradation rate constant, day^{-1}, and t is incubation period, days.

2.7.4. Simulation of ex-situ oil spill remediation

A simulation study was conducted in a glass aquarium containing seawater to evaluate the applicability of the potent composite for remediating oil spills in aquatic ecosystems. The simulation setup consisted of 5 L of Mediterranean seawater, 0.05 L of petroleum, and 0.2 g/L of purified biosurfactant as a surface-active agent to assess the petroleum removal efficiency of the potent composite and its potential application in natural aquatic environments. 10 g of the CH/BNT composite were supplemented for 7 days. The seawater temperature was kept at approximately 25 °C, while its initial pH and salinity conditions were preserved. A single aquarium circulation pump (3W, 1000 L/h) was attached to one side of the glass aquarium to create a dynamic system (Farag et al., 2018; Elkemary et al., 2023).

2.7.5. Long-term experiment

10 g of CH/BNT beads were inoculated into BHB medium prepared at the optimal pH, supplemented with optimal oil and salt concentrations. The incubation was carried out under an optimal temperature condition with shaking at 125 rpm for 7, 14, 21, and 28 days. The percentage of degradation was calculated at 7-day intervals by comparing the weight of oil recovered at each time point to the initial weight measured on day 0. This approach allowed for the assessment of the effects of long-term incubation on both petroleum degradation efficiency and the physical characteristics

of the immobilized bacterial beads (Farid et al., 2024; Liu et al., 2022; Wei et al., 2021).

2.8. Swelling capacities, mechanical stabilities & zero-point charge of CH, CH/GA and CH/BNT

2.8.1. Swelling capacity

1 g of dried CH, CH/GA and CH/BNT beads (W_d) were soaked in distilled water at room temperature. The swollen beads were weighed at certain time intervals until they reached equilibrium (W_s). The percentage of water uptake capacity of the whole beads was calculated using Eq. (5) (Wahba , 2017).

$$\text{SWR}\ (\%) = \frac{[(W_s - W_d)]}{W_d} \times 100\% \quad (5)$$

2.8.2. Mechanical stability

The mechanical stabilities of CH, CH/GA, CH/BNT were compared according to Wahba (2017). After removing excess moisture with filter paper, 0.5 g of beads (W_i) and 1 g of glass beads were vortexed in 1 mL of distilled water for 20 s and then passed through a sieve to remove any broken pieces. The beads remaining on the sieve without disintegration were weighed as W_f. The percentage of mechanical resistance was calculated based on the difference between the initial and final bead weights using Eq. (6).

$$\text{MS}\ (\%) = \left(W_i - W_f\right) \times 100\% \quad (6)$$

2.8.3. Surface zero-point charge

The point of zero charge (pH_{zpc}) of the composite adsorbent was determined using the solid addition method (Mall et al., 2006). A 0.1 M NaCl solution was freshly prepared, and 50 mL aliquots were transferred into a series of 250 mL Erlenmeyer flasks. The initial pH of each solution was adjusted between 2 and 12 using 0.1 M HCl or 0.1 M NaOH, monitored with a calibrated pH meter. 0.1 g of each composite was added to each flask, and the suspensions were agitated to reach equilibrium—ranging from 60 min to 24 h depending on the protocol. Following equilibration, the suspensions were filtered, and the final pH values (pH_f) were recorded. The difference between initial and final pH ($\Delta pH = pH_f - pH_i$) was plotted against the initial pH (pH_i). The point at which ΔpH equals zero was identified as the point of zero charge (pH_{zpc}) of the composite material (Kausar et al., 2019; Olafadehan et al., 2022).

2.9. Characterizations of CH, CH/GA and CH/BNT composites

The thermal stabilities of the CH, CH/GA, and CH/BNT composites, evaluated based on the material's mass change as a function of temperature, were assessed using a Q600 SDT system (simultaneous DSC/TGA) under a nitrogen atmosphere at 10 °C/min from 30 to 800 °C. Fourier Transform Infrared (FT-IR) spectra of the composites were recorded using a Thermo Fisher Nicolet iS50 (USA) spectrophotometer in the range of 4000–400 cm^{-1}. Their surface morphologies were examined with a Focused Ion Beam Scanning Electron Microscope (FIB-SEM; Tescan GAIA3 equipped with an Oxford XMax 150 EDS detector). Prior to imaging, the samples were gold-coated using a Leica ACE 600 coater, and observations were performed at an accelerating voltage of 20 kV (Elashery et al., 2025; Eweida et al., 2023; Ibrahim, 2018; Kausar et al., 2019).

2.10. Statistical analysis

The significance level between the removal efficiencies of free and entrapped consortia and the optimization parameters was calculated using the Kruskal-Wallis H test and Tukey's multiple comparison tests, performed with IBM SPSS® Statistics 23 software. Differences between mean values were considered statistically significant at a 5% confidence level ($p < 0.05$) (Farid et al., 2024; Purnomo et al., 2023).

3. Results and discussion

3.1. Determination of biosurfactant production using bacterial consortium

Microbial strains with suitable metabolic activities must be identified for the simultaneous degradation of hydrocarbons and production of biosurfactants during the bioremediation process (Das and Chandran, 2011; Gaur et al., 2021). Common screening methods for identifying potential biosurfactant producers include the drop-collapse test, oil displacement assay, emulsification index (E_{24}), and surface tension measurement. Among these, the drop-collapse method is a rapid and simple technique that requires only a small sample volume to confirm the presence of biosurfactants (Bodour and Miller-Maier, 1998; Gaur et al., 2021). Similarly, the oil displacement method is a practical and efficient approach, valued for its simplicity, ease of standardization, and time efficiency (Eraqi et al., 2016). This method does not require complex instrumentation and provides quick, reliable results with minimal sample volume (Gaur et al., 2021). As shown in Table 1, the drop collapsed in less than a minute when using the supernatant of the bacterial consortium. The oil displacement measurement with the bacterial consortium was 95.7 ± 4.0 mm. In a comparable study, *Pseudomonas guguanensis* demonstrated an oil spreading diameter of 77.66 ± 0.33 mm. In the present study, the findings from the drop-collapse method were corroborated by the results of the oil displacement assay (Ghazi Faisal et al., 2023). However, Sun et al. (2018) reported that there is no direct correlation between the drop-collapse and oil spreading tests.

Emulsification activity (E_{24}) is a simple, reliable, and rapid method for indicating the presence of biosurfactants. (Nayarisseri et al., 2019). Table 1 shows that the emulsification ability of bacterial consortium was 60.24% with *n*-decane and 40% with *n*-hexadecane. Similarly, Sharma et al. (2015) reported a 64% E_{24} value for *Enterococcus faecium* against kerosene oil. Gaur et al. (2021) obtained that the extracted biosurfactant exhibited a maximum E_{24} of 28.94% ± 0.014% with fresh engine oil, and an E_{24} of approximately 16.0% ± 0.008% with dodecane. In this regard, the emulsification activity depends on the carbon sources used for biosurfactant production (Amani et al., 2013).

3.2. Extraction, purification and characterization of biosurfactant

The cell-free supernatant was acidified to induce precipitation and subsequently extracted with an equal volume of chloroform: methanol (2:1, *v*/*v*) (Fig. 1(a)). The sample was then dried and further analyzed using TLC, a simple and effective technique commonly employed for purifying small quantities of products (Batool et al., 2017). According to the TLC results, the biosurfactant is of a lipopeptide structure, as evidenced by a positive reaction with the ninhydrin reagent, which produced a pink-purple spot indicative of peptide presence. Additionally, a yellow spot was detected due to the reversible reaction of iodine with the lipid moieties in the molecule. The peptide and lipid spots appeared at

Table 1
The screening assays for biosurfactant production by potent bacterial consortium.

Bacterial consortia	[a] Drop-collapse	[b] Oil-spreading, mm	E_{24}, %	
			n-decane	*n*-hexadecane
Bacillus tequilensis & *Bacillus axarquiensis*	+++	95.7 ± 4	60.24	40.0

[a] Change in drop within 1 min (+++).
[b] The diameter of the Petri dish is 110 mm.

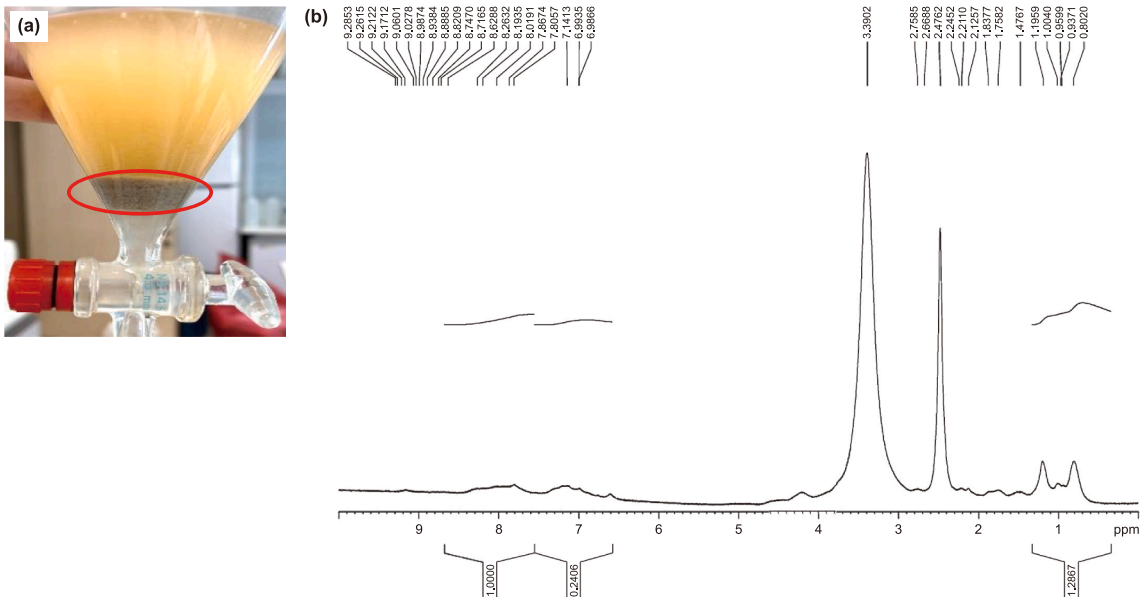

Fig. 1. (**a**) Extraction of biosurfactant; **(b)** ^{1}H NMR analysis of the lipopeptide structure of biosurfactant.

R_f values of 0.61 and 0.63, respectively, consistent with the lipopeptide nature of the biosurfactant. A similar TLC pattern was reported by Sohail and Jamil (2019), who observed R_f values of 0.82 and 0.78 for lipoproteins and free fatty acids produced by *Bacillus tequilensis* MH142145. Fig. 1(b) presents the ^{1}H NMR spectrum of the purified biosurfactant, which clearly confirms its classification as a lipopeptide. This is supported by the presence of signals corresponding to a long aliphatic chain (CH_2) at 1.195 ppm and the peptide backbone (N–H groups) in the region from 8.5 to 7.0 ppm. The sharp peak at 2.476 ppm corresponds to the conjugation between amino acids and fatty acids, while signals between 1.004 and 0.802 ppm correspond to the methyl (CH_3) groups of the fatty acid chains (Cruz et al., 2018; De Faria et al., 2011; Soyuer and Bilen Ozyurek, 2024).

3.3. Comparison of crude oil removal efficiencies by free and entrapped (CH, CH/GA, CH/BNT) biosurfactant-producing consortia

Bioremediation of marine ecosystems contaminated by crude oil and its derivatives, which are known to be carcinogenic, mutagenic, and neurotoxic, is crucial. However, the low solubility of crude oil significantly hinders its degradation. To address this, the use of non-toxic and environmentally friendly surfactants is recommended to enhance oil solubility and bioavailability (Khandelwal et al., 2022). Biosurfactant-producing *Bacillus* sp. strains have been widely used for the remediation of areas contaminated with crude oil. While these strains are highly tolerant to high concentrations of hydrocarbons due to their resistant endospores, they require a prolonged incubation period for growth (Chuah et al., 2022; Costa et al., 2014). Moreover, the loss of microorganisms and the decline in microbial activity over time pose significant challenges for the bioremediation process in marine ecosystems (Luo et al., 2021). This issue can be addressed by immobilizing lipopeptide-producing bacteria on solid surfaces, ensuring a highly stable inoculum with minimal mass transfer limitations (Guo et al., 2021; Khondee et al., 2015). Abdeen et al. (2014) reported that the removal of PAHs by *Bacillus licheniformis* ATCC 10716, *Rhodococcus erythropolis* ATCC 13260, and *Pseudomonas xanthomarina* KMM 1447 was enhanced when these microorganisms were immobilized on crosslinked poly (vinyl alcohol) hydrogel or through biosurfactants produced by free bacterial cells. Biosurfactants produced by free microorganisms and released extracellularly can enhance the biodegradation efficiency of oil (Chen et al., 2017). Cortés-Camargo et al. (2016) reported a biosurfactant production of 1.52 g/L by the free *Bacillus tequilensis* strain. In contrast, the yield of biosurfactant produced by the entrapped consortium in CH/BNT was calculated to be 0.2 g/L. The lower biosurfactant yield in this study, compared to that produced by free microorganisms in the literature, may be attributed to insufficient biosurfactant production in the entrapped cells or the interaction between the biosurfactant and the amino group of chitosan, which inhibits its diffusion into the growth medium (Costa et al., 2014). However, when comparing the petroleum removal efficiencies of the free biosurfactant-producing bacterial consortium and the bacterial consortia entrapped in CH, CH/GA, and CH/BNT matrices, as shown in Fig. 2, the degradation efficiency of the CH/BNT-entrapped consortium was found to be significantly higher than that of the free bacterial consortium. The effectiveness of entrapped-CH/BNT composites in crude oil removal may be attributed to the use of natural clay

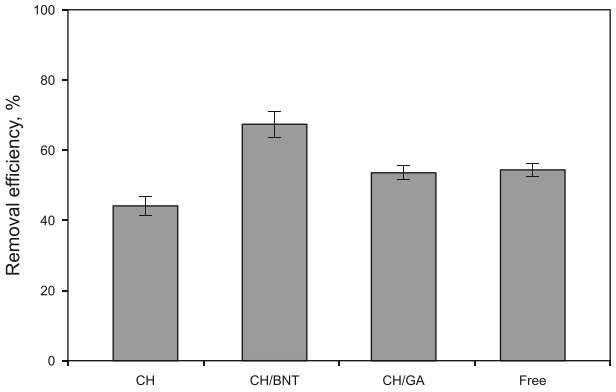

Fig. 2. Comparison of crude oil removal efficiencies of free and immobilized bacterial consortia.

minerals as an alternative to emulsifying agents (Pete et al., 2021). Luo et al. (2021) emphasized the superior oil removal efficiency of immobilized bacterial consortia (*Acinetobacter* sp. Y9, W3, F9, and *Gordonia* sp. X1) over individual bacterial strains, highlighting the limitations of using free cells in the removal process, such as challenges in cell separation from the culture and inefficient substrate transfer to the cells. Similarly, Purnomo et al. (2023) reported that biosurfactant-producing bacteria (*Pseudomonas aeruginosa*, *Bacillus subtilis*, and *Ralstonia pickettii*) immobilized in a PVA/SA/bentonite composite achieved effective hydrocarbon degradation. Likewise, the removal efficiency of naphthalene using the *Bacillus fusiformis* (BFN) strain entrapped in alginate/polyvinyl alcohol/clay beads was significantly higher than that observed with the free BFN strain. This can be attributed to the stabilization of the cell membrane, which aids cell preservation and improves degradation rates. The immobilized beads act as adsorbents around the cells, facilitating degradation by increasing the concentration of available naphthalene (Lin et al., 2014). Furthermore, the large surface area of the beads significantly increases the contact between immobilized microorganisms and crude oil, thereby providing greater opportunities for removal (Farid et al., 2024). The petroleum removal efficiency of the CH/BNT-entrapped bacterial consortium was significantly higher not only than that of the free bacterial consortium but also compared to CH and CH/GA. Statistical analysis confirmed that the removal efficiencies of the CH/BNT-immobilized bacterial consortium were significantly different from those of the other support materials ($p = 0.022$; Table S1). The degradation efficiencies of CH/GA were like those of the free biosurfactant-producing consortium, but higher than those observed for CH (Fig. 2). Statistical analysis confirmed that the degradation efficiencies of the free consortium and the CH/GA-entrapped bacterial consortium were grouped together ($p = 0.022$; Table S1). In a similar study, the enriched crude oil-degrading microbiota entrapped in PVA/SA was found to be more effective in crude oil degradation than both the free and the SA-entrapped microbiota (Huang et al., 2022).

According to the first-order kinetics model equation, the degradation rate constants of bacterial consortia entrapped in CH/BNT, CH/GA, CH, and free bacterial consortium were 1.108, 0.774, 0.576, 0.776 day^{-1}, respectively. The half-life period of entrapped consortia with CH/BNT was notably lower ($t_{1/2} = 0.625$ days) compared with CH/GA ($t_{1/2} = 0.895$ days), CH ($t_{1/2} = 1.203$ days), and free bacterial consortium ($t_{1/2} = 0.893$ days). Accordingly, the low half-life of the entrapped CH/BNT consortium suggests high oil removal efficiency, indicative of elevated microbial activity. Similarly, Warr et al. (2009) reported that clay minerals with a large specific surface area and high cation exchange capacity contribute significantly to bacterial hydrocarbon degradation over time. Similar studies have reported that incorporating bentonite clay improves the removal capacity of entrapped composites (Baigorria et al., 2020; Pandey, 2019). Clay minerals are widely utilized in environmental remediation due to their surface charge, large specific surface area, and interlayer spaces, which enable the efficient removal of both polar and non-polar organic compounds. Their colloidal dimensions not only facilitate the dispersion of oil but also allow the reduction in the size of oil droplets, thereby enhancing the efficiency of oil removal (Farid et al., 2024). Additionally, clay minerals help maintain optimal pH conditions and support bacterial growth by adsorbing protons released during the breakdown of hydrocarbons. Furthermore, the application of clay minerals has expanded to the removal of various anionic contaminants including nitrate, chromate, and arsenate that are toxic to living organisms even at trace levels. However, the inherently negatively charged surfaces of natural clay generally limit their effectiveness for anion adsorption. To overcome this limitation, numerous studies have demonstrated that modifying clays with organic surfactants can transform them into efficient adsorbents, thereby broadening their applicability in environmental remediation (Anjum et al., 2024; Chen et al., 2020; del Mar Orta et al., 2020; Haridharan et al., 2022; Le Quoc et al., 2021; Mokhtar et al., 2024).

To further enhance the performance of CH/BNT composites, future research should explore the integration of activated carbon within the chitosan/bentonite matrix to substantially increase petroleum adsorption capacity (Chen et al., 2020). Additionally, optimizing the physical properties of bentonite through cost-effective acid and thermal treatments can improve matrix porosity and surface chemistry, thereby facilitating enhanced biosurfactant release while maintaining mechanical stability. Acid activation notably increases mesopore volume and overall porosity, augments silanol group density essential for organic compound adsorption, and reduces hydroxyl groups within the clay structure (Pluangklang and Rangsriwatananon, 2021). Alternatively, organic modification of bentonite can reduce its hydrophilicity and alter surface wettability from hydrophilic to organophilic, thereby improving its efficacy in petroleum removal applications (Rostami et al., 2018).

3.4. Statistical design to optimize the main factors affecting petroleum removal by CH/BNT-entrapped consortia

The immobilization of bacteria on a carrier matrix offers numerous advantages, including the provision of a protective niche for long-term microbial survival, enhanced tolerance to variations in pH and temperature, and the potential for reuse of immobilized cells (Berillo et al., 2021; Cortez et al., 2017; Partovinia and Rasekh, 2018; Zommere and Nikolajeva, 2017). In addition, immobilization protects cells from the toxic effects of substrates and reduces the inhibitory effects of various metabolites (Ausheva et al., 2008). In this study, key parameters were optimized to achieve maximum crude oil removal efficiency. These parameters included the amount of Na-bentonite (0.025, 0.05, 0.1, 0.2, and 0.4 g), crude oil concentration (0.25, 0.5, 0.75, and 1 g/50 mL), incubation temperature (20, 25, 30, 35, and 40 °C), initial pH (5.0, 6.0, 7.0, 8.0, and 9.0), salinity (0%, 2.5%, 5%, 7.5%, and 10%), and incubation period (1, 3, 5, 7, and 9 days). These variables were systematically evaluated and adjusted to determine the optimal conditions for maximizing crude oil degradation by CH/BNT-entrapped bacterial consortia. (Fig. 3(a)–(f)).

As shown in Fig. 3(a), the amount of Na-bentonite ranging from 0.025 g to 0.4 g had a significant impact on crude oil removal

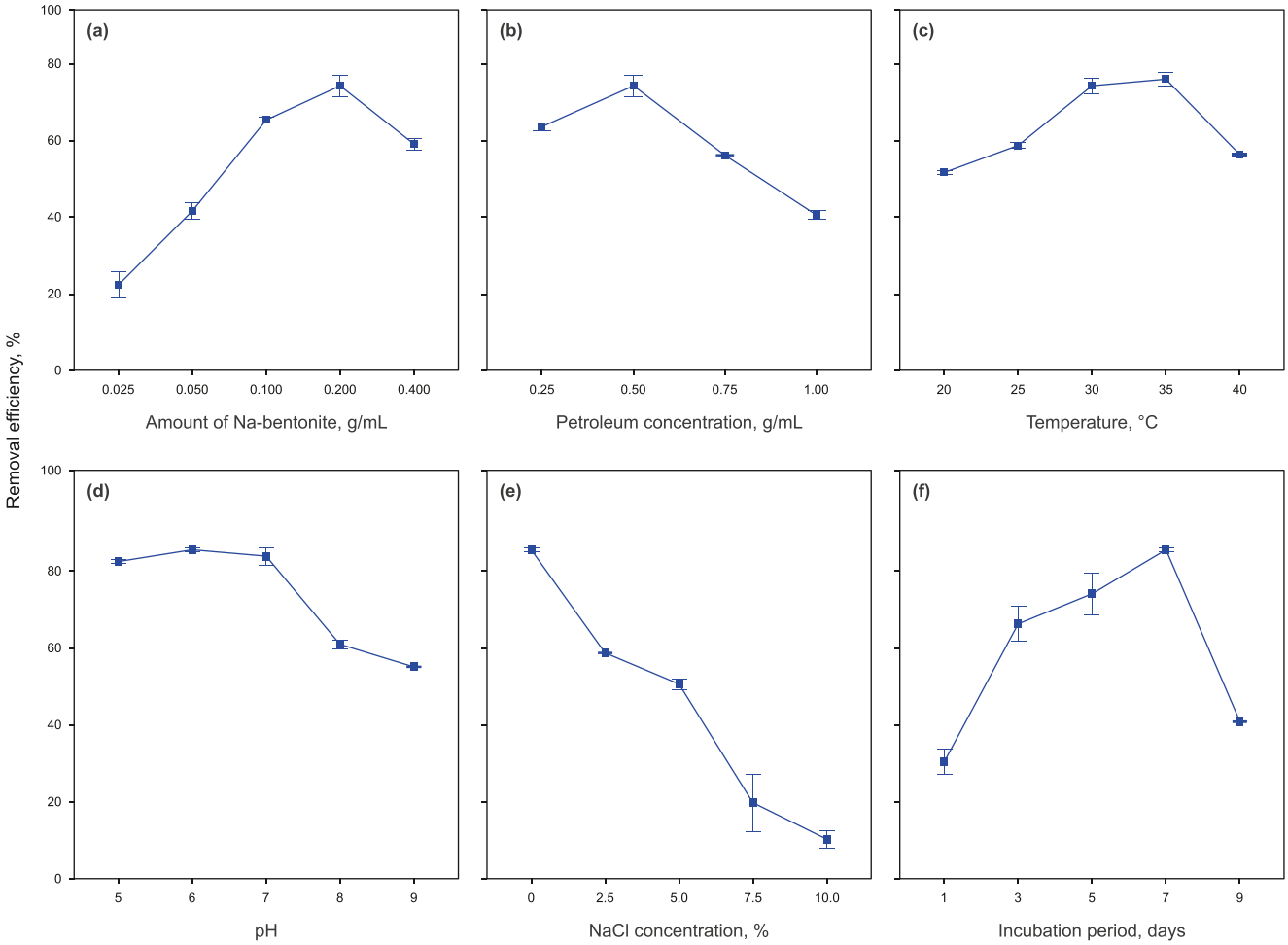

Fig. 3. The effect of the (**a**) amount of Na-bentonite; (**b**) crude oil concentration; (**c**) incubation temperature; (**d**) initial pH; (**e**) salinity; (**f**) incubation period on crude oil removal.

efficiency. Statistical analysis demonstrated that varying the amount of Na-bentonite significantly affected the oil removal capacity of the composite material, with 0.2 g of Na-bentonite yielding the highest removal efficiency ($p = 0.009$; Table S2). While increasing the amount of Na-bentonite up to 0.2 g improved oil removal, a decline in efficiency was observed at 0.4 g. Clay minerals act as structural support, increasing the permeability and porosity of the composite material, thereby promoting microbial activity and facilitating the transport of crude oil into the cells. However, excessive amounts of bentonite may hinder diffusion by obstructing the space required for microbial growth, which could negatively impact the overall degradation process (Lin et al., 2014).

Oil concentration critically affects microbial degradation efficiency, with both low and high levels reducing performance (Chen et al., 2017). In this context, an investigation into the effect of oil concentrations ranging from 0.25 to 1 mL on the removal efficiency by CH/BNT-entrapped consortia revealed that increasing oil concentrations led to a decline in crude oil removal efficiency (Fig. 3(b)). Statistical analysis revealed that an oil concentration of 0.5 mL resulted in a significantly higher removal efficiency compared to all other tested concentrations, highlighting its optimal level for maximizing biodegradation ($p = 0.015$; Table S3). Similarly, Farid et al. (2024) reported that the maximum degradation rates were observed at a 0.5% oil concentration using PVA-alginate-clay composite-entrapped with marine bacteria. Similarly, El-liethy et al. (2022) observed that bacterial growth occurred rapidly at lower oil concentrations but was significantly reduced and suppressed at higher concentrations, with 0.6% identified as the optimal oil concentration for biodegradation. Khandelwal et al. (2022) demonstrated that increasing the oil concentration from 2% to 5% resulted in a decrease in biodegradation efficiency. Consequently, the decline in removal efficiency observed with increasing oil concentration in this study aligns with the results reported in previous research (Abdel-Razek et al., 2020; Abtahi et al., 2020; Chen et al., 2017; Hazim and Al-Ani, 2019).

Temperature affects not only the activity of bacteria but also the physical and chemical properties of crude oil (Chen et al., 2017). In this context, the effect of temperature on oil removal by CH/BNT-entrapped consortia is illustrated in Fig. 3(c). The crude oil removal efficiency of CH/BNT increased from 20 to 35 °C, then decreased at 40 °C. The optimal temperature for maximum oil removal by the bacterial consortia entrapped in CH/BNT was found to be 35 °C. These findings were further validated by statistical analysis ($p = 0.011$; Table S4). Farid et al. (2024) reported that while the maximum oil removal was determined at 30 °C, a decrease was observed at 35 °C. As temperature increases to an optimal level, the bioavailability of microorganisms improves due to enhanced oil solubility. Since microbial growth and enzymatic catalysis are temperature-dependent, increased temperature accelerates microbial metabolism, thereby enhancing oil removal efficiency (Tekere et al., 2019). The bacterial consortium entrapped in CH/

BNT exhibited a removal capacity exceeding 50% even at both the highest (40 °C) and lowest (20 °C) temperatures tested, indicating its ability to adapt to a wide range of oil removal and thus offering broad application potential. Nevertheless, compared to salinity and incubation period, temperature did not cause a dramatic decrease in oil removal. This resilience can be attributed to the fact that the entrapped microorganisms capable of degrading crude oil are indigenous bacterial strains isolated from an oil field, which are naturally adapted to varying environmental conditions (Huang et al., 2017a).

The growth of bacteria in environments with unsuitable pH levels can significantly affect their biodegradation capacity (Venosa and Zhu, 2003). As shown in Fig. 4(d), the oil removal performance of the CH/BNT-entrapped consortia was evaluated across a broad pH range. The results revealed that more than 75% of oil removal was achieved at slightly acidic and neutral pH values, whereas a decline in oil removal efficiency was observed at strongly alkaline pH values. Despite this, the CH/BNT-entrapped consortia exhibited the ability to degrade oil effectively across a wide pH range, with the optimal performance observed at pH = 6.0. Notably, although a decrease in removal efficiency was observed in highly alkaline pH conditions, the consortia still achieved a substantial oil removal rate of over 50% (Fig. 3(d)). This suggests that the bacterial consortia entrapped in CH/BNT retain their stability and oil degradation potential under extreme pH conditions. Statistical analysis confirmed a significant difference in the oil removal efficiencies of the composite at different pH levels ($p = 0.016$; Table S5).

Extreme conditions, such as high salinity, are key factors that limit microbial activity in aquatic ecosystems. In this study, oil removal efficiency by CH/BNT-entrapped consortia decreased significantly from 80.6% to 9.6% as salinity increased (Fig. 3(e)). This effect of NaCl concentration on oil removal efficiency was statistically significant ($p = 0.010$; Table S6). Similarly, Huang et al. (2022) reported that salinity markedly influenced the oil removal efficiencies of both free and immobilized microbiota. Despite the decline at high salinity levels, the CH/BNT composite maintained approximately 50% oil removal at 2.5% and 5% salinity, suggesting that immobilization conferred partial protection to the microorganisms. This protection likely arises from the formation of a compact floc structure between the bacterial consortium and the CH/BNT matrix, which mitigates the inhibitory effects of Na^+ ions and preserves microbial activity. Furthermore, as shown in Fig. 3(f), petroleum removal by the CH/BNT composite increased steadily up to the 7th day, after which a significant decline in removal efficiency occurred. Statistical analysis confirmed the significant influence of incubation period on oil removal ($p = 0.010$; Table S7). The highest oil removal efficiency of 80.5% was achieved at the end of the 7-day incubation period.

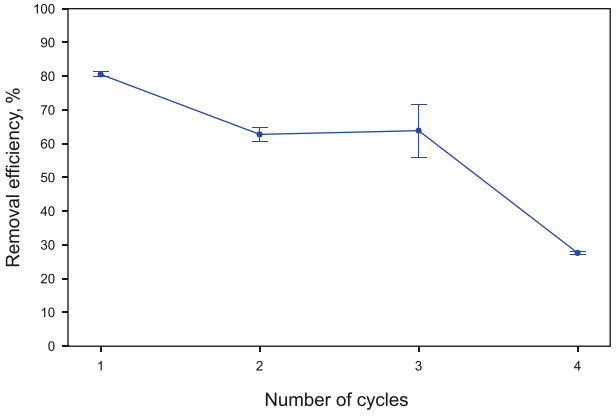

Fig. 4. Reusability of CH/BNT-entrapped consortia on crude oil removal.

3.5. Reusability

The reuse of immobilized bacterial cells enables the maintenance of microbial stability and activity over extended periods, thereby reducing operational costs and enhancing process efficiency (Costa et al., 2014). In this study, although a decline in oil removal efficiency was observed after 7 days of incubation, the removal efficiency remained above 60% during the 2nd and 3rd reuse cycles (Fig. 4). However, a significant reduction in oil removal efficiency was noted after the 4th cycle. These findings were supported by statistical analysis ($p = 0.007$; Table S8). Dotto et al. (2016) reported that chitosan/bentonite hybrid composites could be reused up to three times for the removal of anionic amaranth red and cationic methylene blue dyes. Similarly, the reusability of chitosan/bentonite composites has been demonstrated across various applications, including the removal of dyes, antibiotics, and heavy metals (Elashery et al., 2025; Guo et al., 2023; Majiya et al., 2023). Therefore, this study provides a sustainable approach for the industrial-scale application of environmentally friendly composites by demonstrating the reusability of immobilized beads.

3.6. Simulation study

The application of the CH/BNT composite should extend beyond laboratory-scale studies to include practical implementations for the remediation of oil-polluted water bodies (Senol et al., 2024). Laboratory-scale experiments using seawater provide critical insights into the composite's applicability and scalability, as well as its cost-effectiveness in real-world scenarios. Accordingly, a simulation study was conducted in a glass aquarium under controlled laboratory conditions (Fig. 5(a) and (b)). Compared to the optimized laboratory conditions, the simulation revealed a 20% reduction in petroleum removal efficiency by the CH/BNT composite. Consistent with the optimization results, increased NaCl concentration contributed to decreased petroleum removal efficiency, although the immobilized microorganisms retained partial protection. Additionally, the decline in efficiency may be attributed to a reduction in the mechanical strength of the composite in seawater and insufficient circulation caused by using a single aquarium pump. Therefore, comprehensive investigations are essential to evaluate the properties of spilled oil on the sea surface and at the spill site, alongside assessments of petroleum removal efficiency, reusability, biodegradability, durability, and floatability of the CH/BNT composite under seawater conditions. Such studies are critical to fully assess the composite's potential for large-scale marine oil spill remediation.

3.7. Long-term experiments

As shown in Fig. 6, although a decline in removal efficiency was observed after day 7, approximately 50% petroleum removal was maintained by day 14, with efficiencies around 40% on days 21 and 28. The composite preserved its structural integrity and sustained effective removal performance throughout the extended incubation period. Thus, the efficacy of CH/BNT composites in crude oil removal over a 28-day incubation period has been validated in laboratory studies, positioning them as a promising approach for environmental bioremediation applications.

In alignment with these findings, Baoune et al. (2019) reported a notable decrease in hydrocarbon degradation as after 28 days of

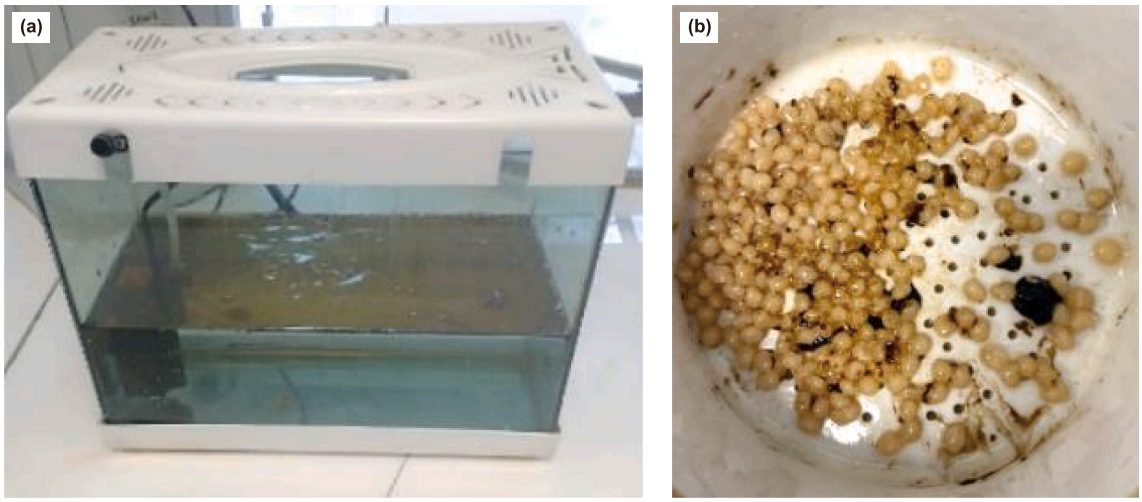

Fig. 5. (**a**) Simulation of crude oil degradation; **(b)** CH/BNT composites exposed to crude oil.

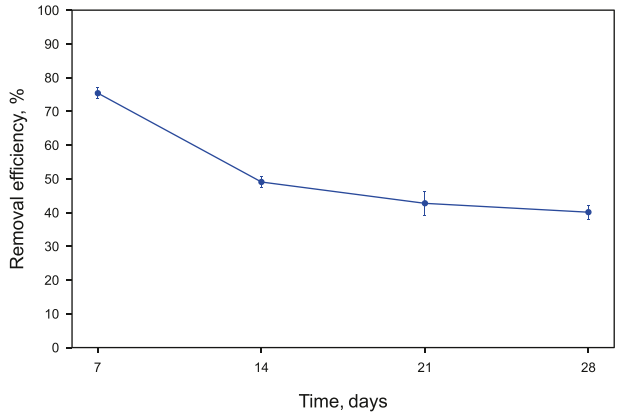

Fig. 6. The removal efficiency of crude oil by CH/BNT composite during a 28-day incubation period.

incubation. Liu et al. (2022) obtained that a bioreactor using immobilized petroleum-degrading bacterial beads achieved over 50% diesel degradation for 27 days. However, degradation efficiency declined over time, coinciding with a 32.5% reduction in bead diameter after 45 days, suggesting that physical changes in the beads may impact long-term bioremediation performance. However, removal efficiencies of embedded degrading bacteria-PVA/alginate/clay composite were 64.7% and 60% at the end of the 7-day incubation, whereas only 76.66% and 70.5% removal efficiencies were attained by the conclusion of the 28-day incubation period (Farid et al., 2024). El-Sheshtawy et al. (2022) reported that the biodegradation percentage enhanced with increasing the incubation time in the degradation of petroleum hydrocarbons using bacterial strains immobilized on goethite-chitosan nanocomposite. A summary of similar contemporary approaches employed for the remediation of petroleum pollution in terrestrial and aquatic ecosystems is presented in Table 2.

3.8. Comparison of mechanical stability, swelling capacity and surface zero-point charge among CH, CH/GA, and CH/BNT composites

This study compared the mechanical stability, swelling capacity and surface zero-point charge of environmentally friendly composites— specifically CH, CH/GA, and CH/BNT. Following vortexing with glass beads for 20 s, the CH, CH/GA, and CH/BNT beads retained 91.49%, 89.47%, and 98.04% of their initial weight, respectively. Wahba (2017) reported that CH/GA activated CP beads retained 75.29% ± 1.90% of their initial weight after similar vortex treatment. These results indicate that the mechanical stability of CH beads is comparable to that of CH/GA beads but inferior to that of CH/BNT beads. Accordingly, Barreto et al. (2010) observed that chitosan beads fragmented during *n*-hexadecane degradation due to chitosanase production by *Bacillus subtilis* LAMI008 encapsulated within chitosan matrix. Therefore, the mechanical stability of chitosan can be enhanced through activation with glutaraldehyde and cross-linking with Na-bentonite. Although CH/BNT beads were prepared without chemical crosslinking agents, Na-bentonite acts as a physical crosslinker, thereby enhancing the mechanical strength of the CH/BNT composite beads (Kamoun and Menzel, 2012). Na-bentonite, a non-toxic and cost-effective material, provides a large surface area and contributes significantly to the mechanical stability of immobilized bacterial cells. Its porous structure facilitates oxygen diffusion, thereby supporting the viability of the bacterial consortium immobilized within the CH/BNT composite (Farid et al., 2024). Additionally, Na-bentonite imparts flexibility to the composite, enabling it to withstand deformation without distortion or damage. Similarly, Benucci et al. (2018) reported that the incorporation of clay enhanced the mechanical properties of nanocomposites. Consequently, compared to CH and CH/GA beads, CH/BNT beads exhibited superior mechanical strength and stiffness, with marked improvements in physical properties such as hardness, durability, and appearance (Kaushal et al., 2018).

The swelling capacity of composites is a critical factor in facilitating effective exchange between immobilized bacteria and their surrounding environment during the bioremediation process. Adequate water uptake is essential to support this exchange. In this study, the water uptake capacities of CH, CH/GA, and CH/BNT beads were compared, as illustrated in Fig. 7. The CH/BNT beads exhibited the highest swelling capacity, which can be attributed to the role of Na-bentonite in enhancing the porosity of the chitosan matrix. Na-bentonite, a clay mineral with a layered, chain-like structure, contains reactive –OH groups on its surface and exchangeable cations within its interlayer channels, contributing to the increased swelling capacity observed (Farid et al., 2024). The elevated number of –OH groups in the CH/BNT composite

Table 2
Summary of recent studies on immobilized biocomposites for petroleum hydrocarbon removal.

Natural-based carriers	Target pollutant	Reference
Bacterial spores entrapped in chitosan beads	Petroleum hydrocarbon	Barreto et al. (2010)
Immobilized calcium alginate/activated carbon	Crude oil	Chen et al. (2017)
Immobilized alginate beads	Oil-contaminated lands	Zommere and Nikolajeva (2017)
Immobilized chitosan-activated carbon	Diesel oil	Muangchinda et al. (2018)
Immobilized alginate–bentonite/guargum–nanobentonite/carboxymethyl cellulose–bentonite	Crude oil	Khandelwal et al. (2022)
Immobilized chitosan/biochar	Crude oil	Liu et al. (2023)
Immobilized PVA/SA/bentonite	Hydrocarbon-contaminated soil	Purnomo et al. (2023)
Immobilized PVA/alginate/clay	Crude oil	Farid et al. (2024)
Immobilized chitosan/Na-bentonite	Crude oil	Present study

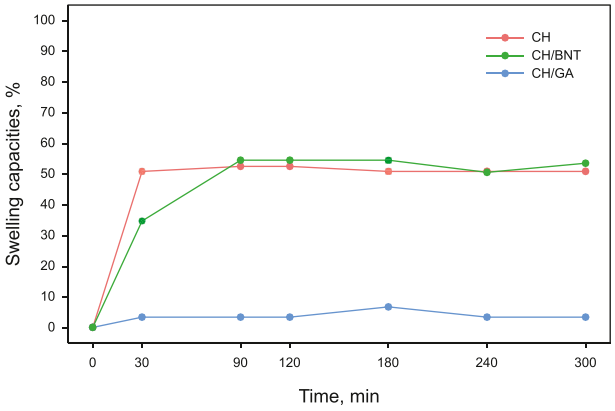

Fig. 7. The swelling capacities of CH, CH/GA, and CH/BNT composites.

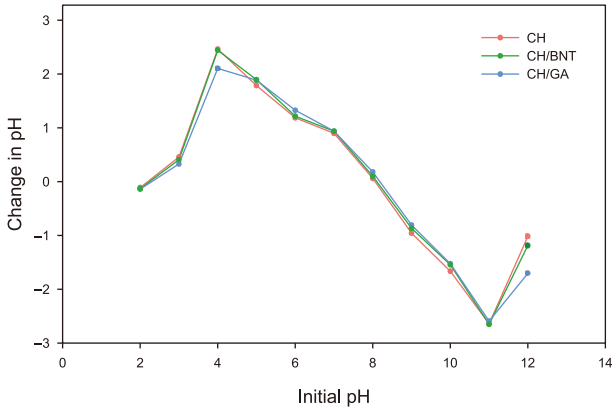

Fig. 8. Zero-point charge of CH, CH/GA, and CH/BNT composites.

enhances its hydrophilicity, resulting in a swelling capacity that surpasses that of the other composites (Knijnenburg et al., 2021). However, the swelling ratios decreased with increasing clay concentration, and 0.25% clay was determined to be the optimal concentration, correlating with the highest degradation rate (Farid et al., 2024). Correspondingly, CH/BNT composite beads containing 0.2 g Na-bentonite, the optimal concentration, demonstrated the greatest mechanical strength and swelling capacity. Bentonite has recently emerged as a promising support material due to its excellent mechanical strength, chemical stability, low cost, and wide availability (Bensalem et al., 2021). Interestingly, while the swelling capacity of inactivated CH was comparable to that of CH/BNT, the swelling capacity of CH/GA beads was significantly lower (Fig. 7). This reduction is consistent with the understanding that lower cross-linker concentrations yield higher swelling capacities but lower mechanical stability, whereas increasing the cross-linker concentration to 3% results in decreased swelling capacity accompanied by enhanced mechanical strength. Thus, although the CH/GA composite prepared with a 2.5% glutaraldehyde solution exhibits relatively high mechanical strength, its swelling capacity remains substantially limited. In summary, the swelling capacity and mechanical stability of CH, CH/GA, and CH/BNT beads exhibited a linear relationship, highlighting the interdependence of these key material properties.

The point of zero charge (pH_{pzc}) of CH, CH/GA, and CH/BNT was determined using the solid addition method to better understand the surface charge characteristics of these materials (Kausar et al., 2019). The surface of the composite becomes negatively charged at pH values above the point of zero charge (pH_{pzc}) and positively charged at pH values below it. As illustrated in Fig. 8, the pH_{pzc} of the CH/BNT composite is ~8.0. Given that the optimal pH for petroleum removal is 7.0, and since pH < pH_{pzc} (i.e., 7.0 < 8.0), the surface of the composite is positively charged under these conditions. At pH 7.0, the CH/BNT composite carries a net positive surface charge, primarily due to the protonation of amino groups ($-NH_3^+$) present in chitosan. This positive surface charge enhances electrostatic attraction and surface interactions with petroleum-based pollutants, thereby improving adsorption efficiency. As the pH increases beyond the pH_{pzc}, the positive surface charge density of both chitosan and bentonite components diminishes, weakening the electrostatic interactions between the composite and negatively charged suspended particles. This reduction leads to a decline in adsorption capacity (Guo et al., 2023; Kausar et al., 2019). Supporting these findings, Anirudhan and Ramachandran (2015) reported a pH_{pzc} of 7.8 for modified clay, while Bée et al. (2017) determined the pH_{pzc} of magnetic chitosan/clay beads to be 7.3.

3.9. Characterization of CH, CH/GA and CH/BNT composites

3.9.1. TGA

Chitosan/bentonite composites typically exhibit significantly enhanced mechanical strength, improved thermal stability, and relatively high surface area (Bensalem et al., 2021). The thermal stability of CS, CS/GA and CH/BNT were evaluated using TGA, as shown in Fig. 9(a), (b), (c), respectively. In the first stage, a weight loss of approximately 10% for CH, CH/GA, and CH/BNT between 30 and 200 °C was observed, which is attributed to the removal of interlayer water molecules and residual acetic acid. A slight mass loss below 250 °C further indicates that the composites possess excellent thermal stability. The second stage involved major mass loss occurring between 250 and 400 °C corresponding to the degradation of chitosan. This degradation is associated with the decomposition of chitosan into CO_2, CO, and H_2O, primarily due to the deacetylation process. For the CH/GA composite, significant mass loss was observed between 280 and 480 °C, which can be

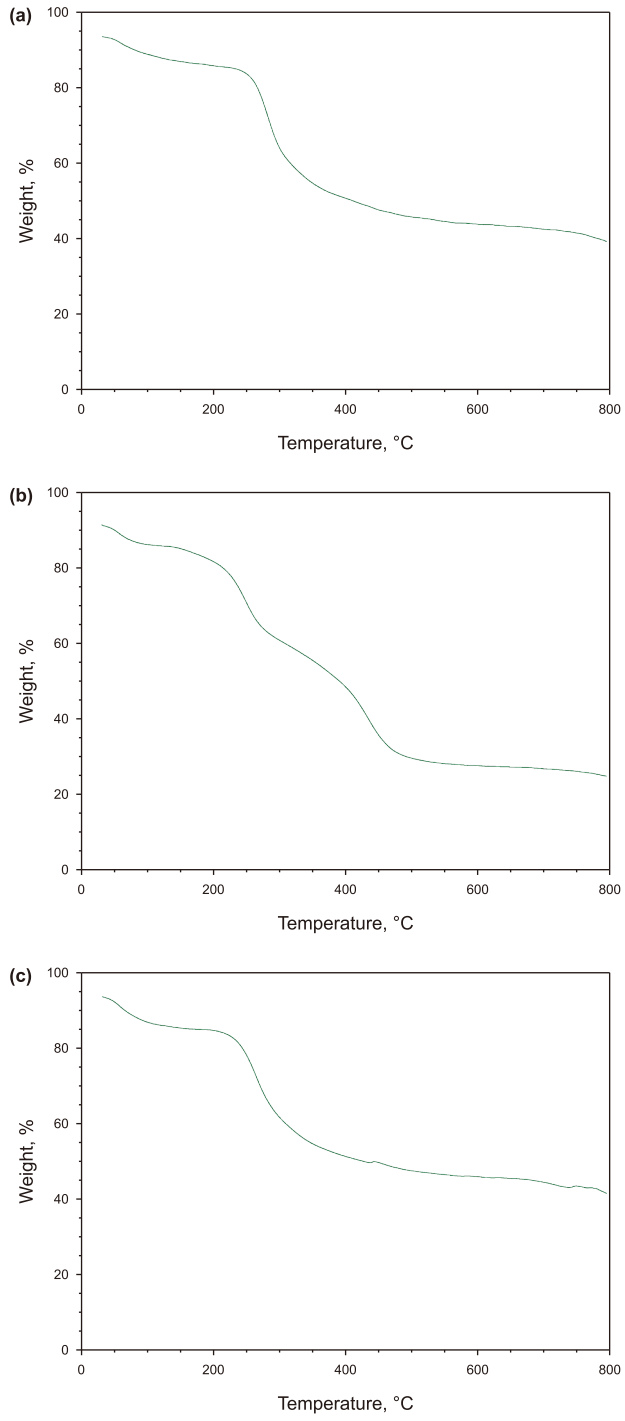

Fig. 9. TG spectra of **(a)** CH; **(b)** CH/GA; **(c)** CH/BNT.

attributed to the decomposition of crosslinked structures formed by glutaraldehyde. The third stage, corresponds to the pyrolysis of the organic components of chitosan.

According to the TG curves, the total mass loss of CH was approximately 45%, whereas the CH/GA composite exhibited a higher mass loss of around 65%. In comparison, the mass loss observed for the CH/BNT composite ranged between 35% and 40%. TGA profiles of CH and CH/BNT composites—both of which exhibited superior mechanical stability and swelling capacity compared to CH/GA—were notably similar. The enhanced thermal stability of the CH/BNT composite can be attributed to the incorporation of Na-bentonite particles, which introduce inorganic components into the organic matrix, thereby increasing resistance to thermal degradation. Overall, these results demonstrate that the CH/BNT composite exhibits enhanced thermal stability (Billah et al., 2024; Guo et al., 2023; Kaur and Kaur, 2024; Kausar et al., 2019).

3.9.2. FT-IR

The identification and characterization of various bonds and linkages present in CH, CH/GA and CH/BNT beads were determined using FT-IR. The FT-IR spectra of CH, CH/GA, and CH/BNT composites after oil treatment were represented as Fig. 10(a), (b), (c). The functional groups were interpreted based on comparisons with similar studies (Abdelnaby et al., 2023; Eraqi et al., 2016; Eweida et al., 2023; Gaur et al., 2021; Kaur and Kaur, 2024; Kaushal et al., 2018; Moussa et al., 2017; Purnomo et al., 2023; Zhu et al., 2023). The FT-IR spectra of CH and CH/GA composites

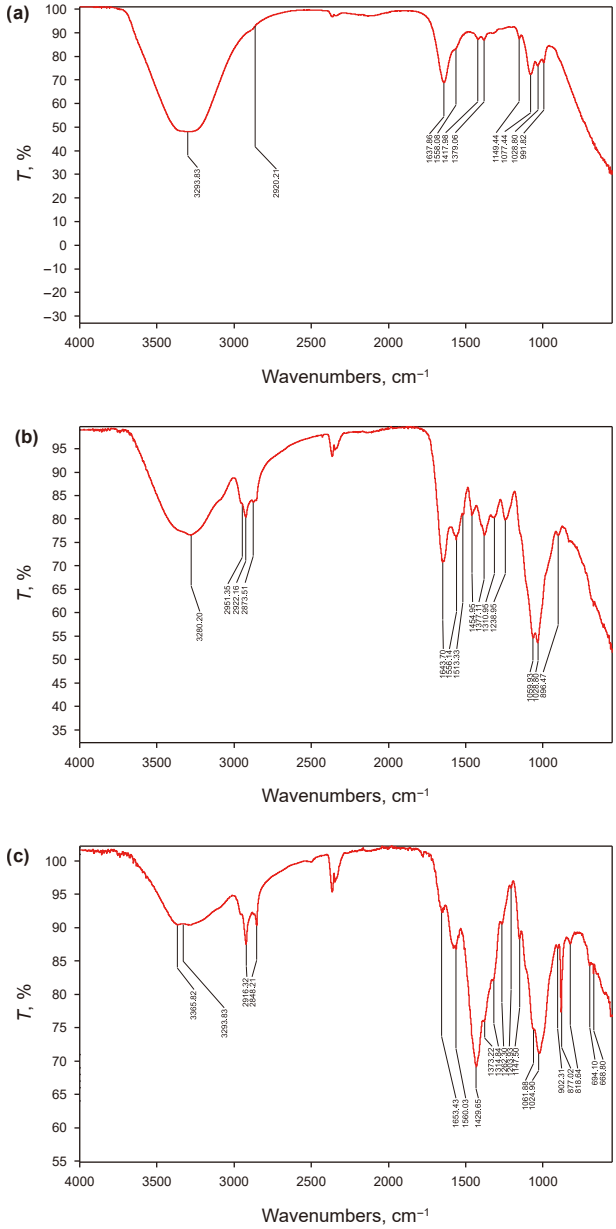

Fig. 10. The FT-IR spectrum of (**a**) CH; (**b**) CH/GA; (**c**) CH/BNT.

exhibit broad bands at 3293 and 3280 cm^{-1}, respectively, attributed to N–H and O–H stretching vibrations. The peak at ~2920 cm^{-1} in CH corresponds to asymmetric CH-stretching, while two nearby bands at 2922 and 2873 cm^{-1} in CH/GA are assigned to asymmetric and symmetric CH_2 stretching vibrations. A sharp peak at 1637 cm^{-1} in CH and 1643 cm^{-1} in CH/GA beads is attributed to the C=O stretching vibration of amide I. A smaller band at 1558 cm^{-1} in CH and 1556 cm^{-1} in CH/GA beads corresponds to the N–H bending of amide II. The peaks at 1379 cm^{-1} in CH and 1377 cm^{-1} in CH/GA are associated with the C–N stretching of amide III. An absorption band at 1149 cm^{-1} in CH corresponds to the asymmetric stretching of the C–O–C bridge. The bands at 1077 and 1028 cm^{-1} in CH, 1059 and 1028 cm^{-1} in CH/GA, are attributed to C–O stretching vibrations. Additionally, the band at 991 cm^{-1} in CH and 896 cm^{-1} in CH/GA is likely due to the amine group of chitosan (Fig. 10(a) and (b)) (Drabczyk et al., 2020; El-araby et al., 2022; Joseph et al., 2016; Queiroz et al., 2015; Salsabila et al., 2024).

The FT-IR spectrum of the CH/BNT composite exhibits characteristic peaks attributable to Na-bentonite. A broad band at 3365 cm^{-1} corresponds to the smectite layer, while an intense band at 1024 cm^{-1} is assigned to the Si–O stretching vibrations of

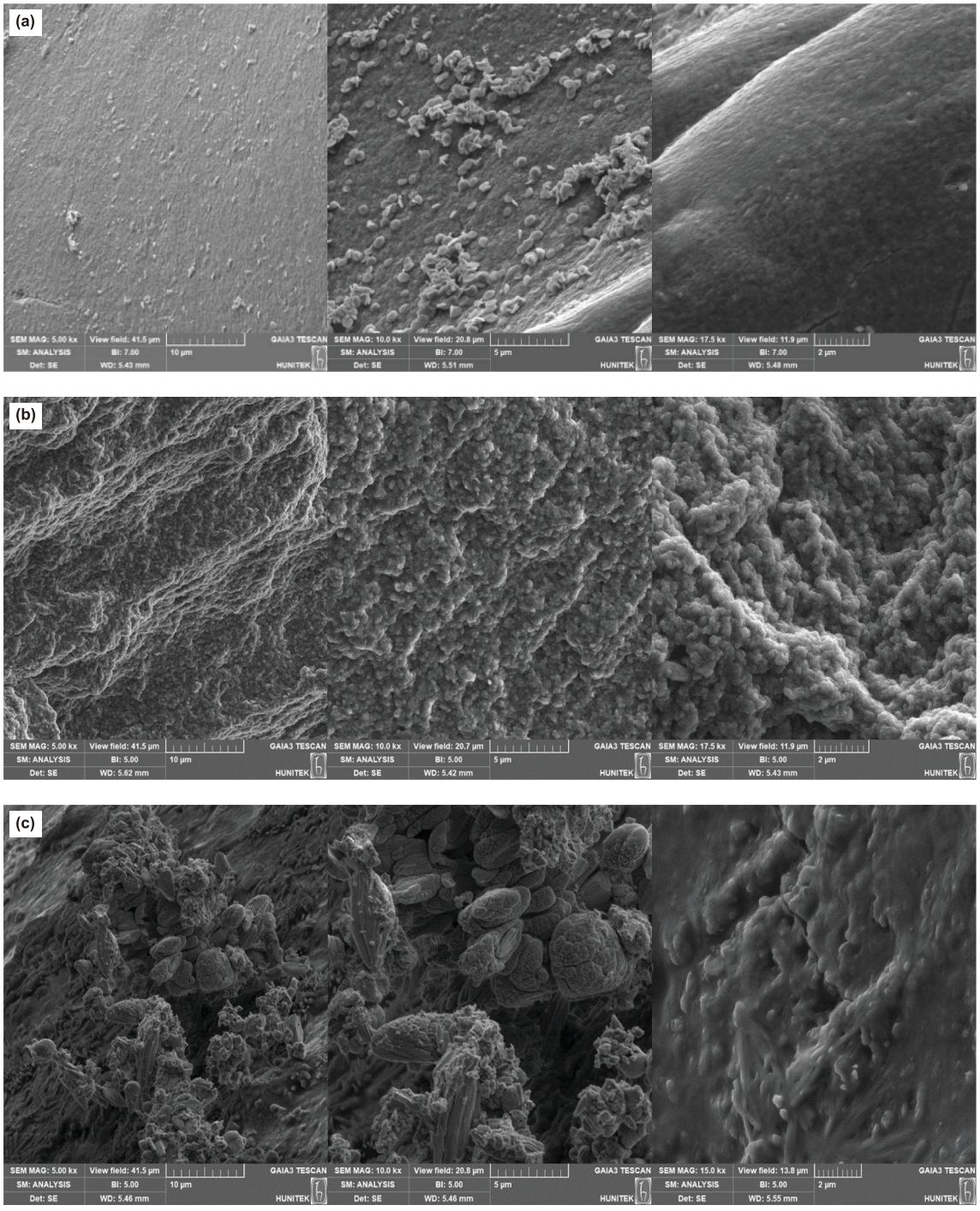

Fig. 11. SEM micrographs of the bacterial consortium entrapped in (**a**) CH, (**b**) CH/GA and (**c**) CH/BNT.

montmorillonite. The band observed at 902 cm^{-1} is associated with octahedral (Al–O–Si) bending vibrations within the smectite structure. Additionally, it shows a characteristic band near 3293 cm^{-1} indicates hydrogen bond formation between the functional groups of chitosan (N–H and O–H) and the O–H groups in bentonite (Fig. 10 (c)). This interaction between chitosan and the Na-bentonite clay layer enhances the number of binding sites in the CH/BNT composite, thereby improving its removal efficiency (Abdel Zaher et al., 2018; Abdelnaby et al., 2023). Consistent with these findings, similar studies have reported that the intercalation of chitosan into the clay layer results in a more effective adsorbent compared to chitosan or clay alone (Guo et al., 2023; Jimtaisong and Sarakonsri, 2019; Majiya et al., 2023).

3.9.3. SEM

The surface morphologies of CH, CH/GA and CH/BNT composites at various magnifications were characterized by SEM, as shown in Fig. 11(a), (b), (c). According to Fig. 11 (a), the surface of CH is non-porous, smooth, and membranous, exhibiting a more compact structure compared to CH/GA and CH/BNT composites. Fig. 11 (b) reveals that CH/GA composites display an uneven, porous surface with heterogeneous pore sizes, characterized by irregular ridges within the bead structure (Zhu et al., 2023). Microorganisms are also visible on the cross-sectional surface of the entrapped beads, which exhibit an irregular morphology containing numerous gaps and channels. According to Fig. 11(c), the CH/BNT composite exhibits a non-porous, clustered, and irregular surface that is notably rougher and more convoluted. Kaya and Ozer (2022) reported similar SEM observations for chitosan-bentonite composites and provided comparable interpretations. The lack of a membranous surface typical of pure chitosan, combined with chitosan's presence within bentonite's porous interlayers, confirms its intercalation into the clay structure. Additionally, chitosan accumulation on the clay's exterior leads to the formation of large pure chitosan lamellae (Rissouli et al., 2025). In conclusion, the chitosan-modified bentonite composite exhibits an uneven surface morphology, which may provide specific binding sites for organic pollutants such as petroleum, thereby enhancing its adsorption capacity (Abdeen et al., 2014; Guo et al., 2024; Kaya and Ozer, 2022; Lin et al., 2014).

4. Conclusion

Immobilization techniques are extensively employed owing to their favorable attributes, including mild reaction conditions, improved mechanical strength, swelling capacity, elevated microbial activity, high cell loading efficiency, and reusability. Among the naturally preferred matrices in immobilization, clay-polymer composites notably enhance critical properties such as mechanical robustness, thermal stability, and porosity. Particularly chitosan/Na-bentonite composites, have emerged as promising materials in bioremediation due to their effective adsorption of diverse pollutants, including petroleum hydrocarbons, heavy metals, nutrients, and dyes. These composites offer a cost-efficient and environmentally sustainable solution for petroleum remediation in aquatic environments, while simultaneously reducing wastewater treatment costs. Based on the comparative analysis conducted, the key conclusions are as follows:

(1) The biosurfactants produced by the *Bacillus tequilensis* and *Bacillus axarquiensis* consortium were confirmed to possess a lipopeptide structure.
(2) The petroleum removal efficiency of the CH/BNT-entrapped bacterial consortium was significantly superior to both the free bacterial consortium and the CH and CH/GA composites.
(3) Maximum crude oil removal was achieved using 0.5 mL of crude oil with the CH/BNT composite containing 0.1 g of Na-bentonite at pH = 6.0 and 35 °C over a 7-day incubation period. Additionally, oil removal efficiency declined with increasing salinity.
(4) Although the removal efficiency remained above 50% during the 2nd and 3rd incubation cycles, a pronounced decrease in oil removal was noted after the 4th cycle.
(5) The interaction between chitosan and the Na-bentonite clay layer enhances the number of binding sites within the CH/BNT composite, thereby improving its removal efficiency.
(6) The CH/BNT composite exhibited superior mechanical stability, swelling capacity, and thermal stability compared to CH and CH/GA composites.
(7) The efficacy of CH/BNT composites for crude oil removal has been conclusively demonstrated through both 28-day laboratory experiments and laboratory-scale simulation studies.
(8) The CH/BNT composite has a point of zero charge near pH = 8.0, and its positive surface charge at pH = 7.0 enhances petroleum pollutant adsorption via increased electrostatic attraction, a key factor for advancing adsorption research.
(9) Overall, the CH/BNT composite is a cost-effective, eco-friendly, and recyclable material with significant potential for sustainable bioremediation of oil pollution in aquatic ecosystems. Beyond oil remediation, CH/BNT-based materials are also expected to effectively remove various industrial pollutants, including heavy metals and textile dyes, from an aquatic environment.
(10) While laboratory and simulation studies have validated the efficacy of the CH/BNT composite, future research should focus on addressing critical challenges to facilitate practical application. These include evaluating the effects of environmental variability, enhancing long-term stability and reusability, and conducting advanced pilot-scale and in-situ field trials. Such efforts are crucial to validate laboratory results and optimize deployment strategies under complex real-world conditions.

CRediT authorship contribution statement

Sezen Bilen Ozyurek: Writing – review & editing, Writing – original draft, Supervision, Project administration, Methodology, Data curation, Conceptualization. **Kaan Soyuer:** Visualization, Validation, Software, Data curation. **Arda Ustundag:** Writing – review & editing, Software, Investigation.

Data availability

All data generated or analyzed during this study are included in this published article (and its supplementary information files).

Declaration of competing interest

The authors declare that they have no known competing financial interests or personal relationships that could have appeared to influence the work reported in this paper.

Appendix A. Supplementary data

Supplementary data to this article can be found online at https://doi.org/10.1016/j.petsci.2025.09.039.

References

Abdeen, Z., El-Sheshtawy, H.K., Moustafa, Y.M.M., 2014. Enhancement of crude oil biodegradation by immobilizing different bacterial strains on porous PVA hydrogels or combining of them with their produced biosurfactants. J. Petrol Environ. Biotechnol. 5 (5), 1. https://doi.org/10.4172/2157-7463.1000192.

Abdelnaby, A., Abdelaleem, N.M., Elshewy, E., Mansour, A.H., Ibrahim, S.S., 2023. Application of bentonite clay, date pit, and chitosan nanoparticles as promising adsorbents to sequester toxic lead and cadmium from milk. Biol. Trace Elem. Res. 201 (5), 2650–2664. https://doi.org/10.1007/s12011-022-03353-w.

Abdel-Razek, A.S., El-Sheikh, H.H., Suleiman, W.B., Taha, T.H., Mohamed, M.K., 2020. Bioelimination of phenanthrene using degrading bacteria isolated from petroleum soil: safe approach. Desalination Water Treat. 181, 131–140. https://doi.org/10.5004/dwt.2020.25109.

Abdel-Zaher, M.S., Abdel Wahab, S.M., Taha, M.H., Masoud, A.M., 2018. Sorption characteristics of iron, fluoride and phosphate from wastewater of phosphate fertilizer plant using natural sodium bentonite. J. Membr. Sci. Technol. 8 (2), 1–10. https://doi.org/10.4172/2155-9589.1000186.

Abtahi, H., Parhamfar, M., Saeedi, R., Villasenor, J., Sartaj, M., Kumar, V., Coulon, F., Parhamfar, M., Didehdar, M., Seifi, H., Koolivand, A., 2020. Effect of competition between petroleum-degrading bacteria and Indigenous compost microorganisms on the efficiency of petroleum sludge bioremediation: field application of mineral-based culture in the composting process. J. Environ. Manag. 258, 110013. https://doi.org/10.1016/j.jenvman.2019.110013.

Abulimiti, M., Wang, J., Li, C., Zhang, Y., Li, S., 2023. Bentonite could be an eco-friendly windbreak and sand-fixing material. Environ. Technol. Innov. 29, 102981. https://doi.org/10.1016/j.eti.2022.102981.

Alexander, J.A., Ahmad, Zaini, M.A., Surajudeen, A., Aliyu, E.N.U., Omeiza, A.U., 2019. Surface modification of low-cost bentonite adsorbents—A review. Part. Sci. Technol. 37 (5), 538–549. https://doi.org/10.1080/02726351.2018.1438548.

Ali, N., Dashti, N., Khanafer, M., Al-Awadhi, H., Radwan, S., 2020. Bioremediation of soils saturated with spilled crude oil. Sci. Rep. 10 (1), 1116. https://doi.org/10.1038/s41598-019-57224-x.

Amani, H., Müller, M.M., Syldatk, C., Hausmann, R., 2013. Production of microbial rhamnolipid by *Pseudomonas aeruginosa* MM1011 for ex-situ enhanced oil recovery. Appl. Biochem. Biotechnol. 170, 1080–1093. https://doi.org/10.1007/s12010-013-0249-4.

Anirudhan, T., Ramachandran, M., 2015. Adsorptive removal of basic dyes from aqueous solutions by surfactant modifiedbentonite clay (organoclay): kinetic and competitiveadsorption isotherm. Process. Saf. Environ. Protect. 95, 215–225.

Anjum, A., Gupta, D., Singh, B., Garg, R., Pani, B., Kashif, M., Jain, S., 2024. Clay–polymer nanocomposites for effective water treatment: Opportunities, challenges, and prospects. Environ. Monit. Assess. 196 (7), 666. https://doi.org/10.1007/s10661-024-12823-8.

Aragaw, T.A., 2021. Functions of various bacteria for specific pollutants degradation and their application in wastewater treatment: A review. Int. J. Environ. Sci. Technol. 18, 2063–2076. https://doi.org/10.1007/s13762-020-03022-2.

Ausheva, K.A., Goncharuk, D.A., Babusenko, E.S., Nekhaev, S.A., Sultygova, Z.S., Markvichev, N.S., 2008. Development of bacterial preparation based on immobilized cells. Theor. Found. Chem. Eng. 42, 767–773. https://doi.org/10.1134/s0040579508050503.

Baigorria, E., Cano, L.A., Sanchez, L.M., Alvarez, V.A., Ollier, R.P., 2020. Bentonite-composite polyvinyl alcohol/alginate hydrogel beads: preparation, characterization, and their use as arsenic removal devices. Environ. Nanotechnol. Monit. Manag. 14, 100364. https://doi.org/10.1016/j.enmm.2020.100364.

Balan, S.S., Kumar, C.G., Jayalakshmi, S., 2016. Pontifactin, a new lipopeptide biosurfactant produced by a marine *Pontibacter korlensis* strain SBK-47: purification, characterization and its biological evaluation. Process Biochem. 51 (12), 2198–2207. https://doi.org/10.1016/j.procbio.2016.09.009.

Barreto, R.V.G., Hissa, D.C., Paes, F.A., Grangeiro, T.B., Nascimento, R.F., Rebelo, L.M., Craveiro, A.A., Melo, V., 2010. New approach for petroleum hydrocarbon degradation using bacterial spores entrapped in chitosan beads. Bioresour. Technol. 101 (7), 2121–2125. https://doi.org/10.1016/j.biortech.2009.11.004.

Batool, R., Ayub, S., Akbar, 2017. Isolation of biosurfactant producing bacteria from petroleum contaminated sites and their characterization. Soil. Environ. Times 36 (1), 35–44. https://doi.org/10.25252/se/17/20992.

Baoune, H., Aparicio, J.D., Pucci, G., Ould El Hadj-Khelil, A., Polti, M.A., 2019. Bioremediation of petroleum-contaminated soils using streptomyces sp. Hlh1. J. Soils Sediments 19, 2222–2230. https://doi.org/10.1007/s11368-019-02259-w.

Bée, A., Obeid, L., Mbolantenaina, R., Welschbillig, M., Talbot, D., 2017. Magnetic chitosan/clay beads: A magsorbent for the removal of cationic dye from water. J. Magn. Magn Mater. 421, 59–64. https://doi.org/10.1016/j.jmmm.2016.07.022.

Belousov, P., Chupalenkov, N., Christidis, G.E., Zakusina, O., Zakusin, S., Morozov, I., Chernov, M., Zaitsava, T., Tyupina, E., Krupskaya, V., 2021. Carboniferous bentonites from 10Th Khutor deposit (Russia): Composition, properties and features of genesis. Appl. Clay Sci. 215, 106308. https://doi.org/10.1016/j.clay.2021.106308.

Benucci, I., Liburdi, K., Cacciotti, I., Lombardelli, C., Zappino, M., Nanni, F., Esti, M., 2018. Chitosan/clay nanocomposite films as supports for enzyme immobilization: An innovative green approach for winemaking applications. Food Hydrocoll. 74, 124–131. https://doi.org/10.1016/j.foodhyd.2017.08.005.

Bensalem, S., Hamdi, B., Del Confetto, S., Calvet, R., 2021. Characterization of surface properties of chitosan/bentonite composites beads by inverse gas chromatography. Int. J. Biol. Macromol. 166, 1448–1459. https://doi.org/10.1016/j.ijbiomac.2020.11.024.

Berillo, D., Al-Jwaid, A., Caplin, J., 2021. Polymeric materials used for immobilisation of bacteria for the bioremediation of contaminants in water. Polymers 13 (7), 1073. https://doi.org/10.3390/polym13071073.

Bilen Ozyurek, S., Seyis Bilkay, I., 2017. Determination of petroleum biodegradation by bacteria isolated from drilling fluid, waste mud pit and crude oil. Turk. J. Biochem. 42 (6), 609–616. https://doi.org/10.1515/tjb-2017-0087.

Bilen Ozyurek, S., Seyis Bilkay, I., 2020. Comparison of petroleum biodegradation efficiencies of three different bacterial consortia determined in petroleum-contaminated waste mud pit. SN Appl. Sci. 2, 1–12. https://doi.org/10.1007/s42452-020-2044-5.

Billah, R.E.K., Islam, M.A., Nazal, M.K., Bahsis, L., Soufiane, A., Abdellaoui, Y., Achak, M., 2024. A novel glutaraldehyde cross-linked chitosan@ acid-activated bentonite composite for effective Pb (II) and Cr (VI) adsorption: experimental and theoretical studies. Sep. Purif. Technol. 334, 126094. https://doi.org/10.1016/j.seppur.2023.126094.

Bodour, A.A., Miller-Maier, R.M., 1998. Application of a modified drop-collapse technique for surfactant quantitation and screening of biosurfactant-producing microorganisms. J. Microbiol. Methods 32 (3), 273–280. https://doi.org/10.1016/s0167-7012(98)00031-1.

Cengiz, S., Çavaş, L., Yurdakoç, K., 2012. Bentonite and sepiolite as supporting media: immobilization of catalase. Appl. Clay Sci. 65, 114–120. https://doi.org/10.1016/j.clay.2012.06.004.

Chaurasia, L.K., Tamang, B., Tirwa, R.K., Lepcha, P.L., 2020. Influence of biosurfactant producing *Bacillus tequilensis* LK5. 4 isolates of kinema, a fermented soybean, on seed germination and growth of maize (Zea mays L.). 3 Biotech 10, 1–12. https://doi.org/10.1007/s13205-020-02281-7.

Chen, Q., Li, J., Liu, M., Sun, H., Bao, M., 2017. Study on the biodegradation of crude oil by free and immobilized bacterial consortium in marine environment. PLoS One 12 (3), e0174445. https://doi.org/10.1371/journal.pone.0174445.

Chen, H., Zheng, K., Zhu, A., Meng, Z., Li, W., Qin, C., 2020. Preparation of bentonite/chitosan composite for bleaching of deteriorating transformer oil. Polymers 12 (1), 60. https://doi.org/10.3390/polym12010060.

Chettri, B., Singha, N.A., Singh, A.K., 2021. Efficiency and kinetics of Assam crude oil degradation by *Pseudomonas aeruginosa* and *Bacillus sp.* Arch. Microbiol. 203, 5793–5803. https://doi.org/10.1007/s00203-021-02567-1.

Chuah, L.F., Chew, K.W., Bokhari, A., Mubashir, M., Show, P.L., 2022. Biodegradation of crude oil in seawater by using a consortium of symbiotic bacteria. Environ. Res. 213, 113721. https://doi.org/10.1016/j.envres.2022.113721.

Cortés-Camargo, S., Pérez-Rodríguez, N., de Souza Oliveira, R.P., Huerta, B.E.B., Domínguez, J.M., 2016. Production of biosurfactants from vine-trimming shoots using the halotolerant strain *Bacillus tequilensis* ZSB10. Ind. Crop. Prod. 79, 258–266. https://doi.org/10.1016/j.indcrop.2015.11.003.

Cortez, S., Nicolau, A., Flickinger, M.C., Mota, M., 2017. Biocoatings: A new challenge for environmental biotechnology. Biochem. Eng. J. 121, 25–37. https://doi.org/10.1016/j.bej.2017.01.004.

Costa, S.P., Angelim, A.L., de Queiroz, M.D.F.V., Melo, V.M.M., 2014. Vegetative cells of *Bacillus pumilus* entrapped in chitosan beads as a product for hydrocarbon biodegradation. Int. Biodeterior. Biodegrad. 87, 122–127. https://doi.org/10.1016/j.ibiod.2013.11.011.

Cruz, J.M., Hughes, C., Quilty, B., Montagnolli, R.N., Bidoia, E.D., 2018. Agricultural feedstock supplemented with manganese for biosurfactant production by *Bacillus subtilis*. Waste Biomass Valor 9, 613–618. https://doi.org/10.1007/s12649-017-0019-6.

Das, N., Chandran, P., 2011. Microbial degradation of petroleum hydrocarbon contaminants: an overview. Biotechnol. Res. Int. 2011 (1), 941810. https://doi.org/10.4061/2011/941810.

De Almeida, D.G., Soares Da Silva, R.D.C.F., Luna, J.M., Rufino, R.D., Santos, V.A., Banat, I.M., Sarubbo, L.A., 2016. Biosurfactants: promising molecules for petroleum biotechnology advances. Front. Microbiol. 7, 230300. https://doi.org/10.3389/fmicb.2016.01718.

De Faria, A.F., Teodoro-Martinez, D.S., de Oliveira Barbosa, G.N., Vaz, B.G., Silva, Í.S., Garcia, J., Tótola, M.R., Eberlin, M.N., Grossman, M., Alves, O.L., Durrant, L.R., 2011. Production and structural characterization of surfactin (C14/Leu7) produced by *Bacillus subtilis* isolate LSFM-05 grown on raw glycerol from the biodiesel industry. Process Biochem. 46 (10), 1951–1957. https://doi.org/10.1016/j.procbio.2011.07.001.

del Mar Orta, M., Martín, J., Santos, J.L., Aparicio, I., Medina-Carrasco, S., Alonso, E., 2020. Biopolymer-clay nanocomposites as novel and ecofriendly adsorbents for environmental remediation. Appl. Clay Sci. 198, 105838. https://doi.org/10.1016/j.clay.2020.105838.

Dotto, G.L., Rodrigues, F.K., Tanabe, E.H., Fröhlich, R., Bertuol, D.A., Martins, T.R., Foletto, E.L., 2016. Development of chitosan/bentonite hybrid composite to remove hazardous anionic and cationic dyes from colored effluents. J. Environ. Chem. Eng. 4 (3), 3230–3239. https://doi.org/10.1016/j.jece.2016.07.004.

Dotto, J., Espinoza-Quiñones, F.R., Milinsk, M.C., Alves, H.J., 2021. High performance on the moisture reduction in waste oils by a bentonite-based adsorption process. Environ. Technol. 42 (21), 3338–3347. https://doi.org/10.1080/09593330.2020.1728391.

Drabczyk, A., Kudłacik-Kramarczyk, S., Głąb, M., Kędzierska, M., Jaromin, A., Mierzwiński, D., Tyliszczak, B., 2020. Physicochemical investigations of

chitosan-based hydrogels containing aloe vera designed for biomedical use. Materials 13 (14), 3073. https://doi.org/10.3390/ma13143073.
El-araby, A., El Ghadraoui, L., Errachidi, F., 2022. Usage of biological chitosan against the contamination of post-harvest treatment of strawberries by *Aspergillus niger*. Front. Sustain. Food Syst. 6, 881434. https://doi.org/10.3389/fsufs.2022.881434.
Elashery, S.E., El-Bouraie, M.M., Abdelgawad, E.A., Attia, N.F., Mohamed, G.G., 2025. Adsorptive performance of bentonite-chitosan nanocomposite as a dual antibacterial and reusable adsorbent for Reactive Red 195 and crystal violet removal: kinetic and thermodynamic studies. Biomass Convers. Biorefin. 1-14. https://doi.org/10.1007/s13399-023-05059-y.
El-liethy, M.A., El-Noubi, M.M., Abia, A.L.K., El-Malky, M.G., Hashem, A.I., El-Taweel, G.E., 2022. Eco-friendly bioremediation approach for crude oil-polluted soils using a novel and biostimulated *Enterobacter hormaechei* ODB H32 strain. Int. J. Environ. Sci. Technol. 19 (11), 10577–10588. https://doi.org/10.1007/s13762-021-03885-z.
Elkemary, A., Abouelkheir, S.S., Abdel Hakim, M., Sabry, S.A., Ghozlan, H.A., 2023. Potential Egyptian bacterial consortium for oil spill treatment: a laboratory simulation. Case Stud. Chem. Environ. Eng. 7, 100278. https://doi.org/10.1016/j.cscee.2022.100278.
El-Sheshtawy, H., Aman, D., Nassar, H., 2022. A novel bioremediation technique for petroleum hydrocarbons by bacterial consortium immobilized on goethite-chitosan nanocomposite. Soil Sediment Contam. 31, 176–199.
Eraqi, W.A., Yassin, A.S., Ali, A.E., Amin, M.A., 2016. Utilization of crude glycerol as a substrate for the production of rhamnolipid by *Pseudomonas aeruginosa*. Biotechnol. Res. Int. 2016 (1), 3464509. https://doi.org/10.1155/2016/3464509.
Eweida, B.Y., Omer, A.M., Tamer, T.M., Soliman, H.A.E.M., Zaatot, A.A., Mohy-Eldin, M.S., 2023. Kinetics, isotherms, and thermodynamics of oil spills removal by novel amphiphilic Chitosan-g-Octanal Schiff base polymer developed by click grafting technique. Polym. Bull. 80 (5), 4813–4840. https://doi.org/10.1007/s00289-022-04260-9.
Farag, S., Soliman, N.A., Abdel-Fattah, Y.R., 2018. Enhancement of crude oil biodegradation by immobilized bacterial consortium in small batch and continuous bioreactor modes. Egypt. J. Chem. 61 (6), 1019–1030. https://doi.org/10.21608/ejchem.2018.3820.1336.
Farid, E., Kamoun, E.A., Taha, T.H., El-Dissouky, A., Khalil, T.E., 2024. Eco-friendly biodegradation of hydrocarbons compounds from crude oily wastewater using PVA/alginate/clay composite hydrogels. J. Polym. Environ. 32 (1), 225–245. https://doi.org/10.1007/s10924-023-02991-y.
Ferhat, M., Kadouche, S., Drouiche, N., Messaoudi, K., Messaoudi, B., Lounici, H., 2016. Competitive adsorption of toxic metals on bentonite and use of chitosan as flocculent coagulant to speed up the settling of generated clay suspensions. Chemosphere 165, 87–93. https://doi.org/10.1080/13102818.2017.1309992.
Gaur, S., Gupta, S., Jain, A., 2021. Characterization and oil recovery application of biosurfactant produced during bioremediation of waste engine oil by strain *Pseudomonas aeruginosa* gi| KP 16392| isolated from Sambhar Salt Lake. Biorem. J. 25 (4), 308–325. https://doi.org/10.1080/10889868.2020.1871316.
Ghazi Faisal, Z., Sallal Mahdi, M., Alobaidi, K.H., 2023. Optimization and chemical characterization of biosurfactant produced from a novel *Pseudomonas guguanensis* strain Iraqi ZG. KM. Internet J. Microbiol. https://doi.org/10.1155/2023/1571991, 2023.
Goveas, L.C., Selvaraj, R., Sajankila, S.P., 2022. Characterization of biosurfactant produced in response to petroleum crude oil stress by *Bacillus sp.* WD22 in marine environment. Braz. J. Microbiol. 53 (4), 2015–2025. https://doi.org/10.1007/s42770-022-00811-4.
Guo, J., Chen, C., Chen, W., Jiang, J., Chen, B., Zheng, F., 2021. Effective immobilization of *Bacillus subtilis* in chitosan-sodium alginate composite carrier for ammonia removal from anaerobically digested swine wastewater. Chemosphere 284, 131266. https://doi.org/10.1016/j.chemosphere.2021.131266.
Guo, X., Wu, Z., Wang, Z., Lin, F., Li, P., Liu, J., 2023. Preparation of chitosan-modified bentonite and its adsorption performance on tetracycline. ACS Omega 8 (22), 19455–19463. https://doi.org/10.1021/acsomega.3c00745.
Guo, X., Wu, Z., Lu, Z., Wang, Z., Li, S., Madhau, F., Huo, R., 2024. Preparation and characterization of chitosan-modified bentonite hydrogels and application for tetracycline adsorption from aqueous solution. Gels 10 (8), 503. https://doi.org/10.3390/gels10080503.
Gur, S.D., İdil, N., Aksöz, N., 2018. Optimization of enzyme co-immobilization with sodium alginate and glutaraldehyde-activated chitosan beads. Appl. Biochem. Biotechnol. 184, 538–552. https://doi.org/10.1007/s12010-017-2566-5.
Haridharan, N., Sundar, D., Kurrupasamy, L., Anandan, S., Liu, C.H., Wu, J.J., 2022. Oil spills adsorption and cleanup by polymeric materials: a review. Polym. Adv. Technol. 33 (5), 1353–1384. https://doi.org/10.1002/pat.5636.
Hazaimeh, M., Abd Mutalib, S., Abdullah, P.S., Kok Kee, W., Surif, S., 2014. Enhanced crude oil hydrocarbon degradation by self-immobilized bacterial consortium culture on sawdust and oil palm empty fruit bunch. Ann. Microbiol. 64, 1769–1777. https://doi.org/10.1007/s13213-014-0821-3.
Hazim, R.N., Al-Ani, M.A., 2019. Effect of petroleum hydrocarbons contamination on soil microorganisms and biodegradation. Raf. J. Sci. 13-22. https://doi.org/10.33899/rjs.2019.159391.
Huang, X., Bai, J., Li, K.R., Zhao, Y.G., Tian, W.J., Dang, J.J., 2017. Characteristics of two novel cold-and salt-tolerant ammonia-oxidizing bacteria from Liaohe Estuarine Wetland. Mar. Pollut. Bull. 114 (1), 192–200. https://doi.org/10.1016/j.marpolbul.2016.08.077.
Huang, Y., Pan, H., Wang, Q., Ge, Y., Liu, W., Christie, P., 2019. Enrichment of the soil microbial community in the bioremediation of a petroleum-contaminated soil amended with rice straw or sawdust. Chemosphere 224, 265–271. https://doi.org/10.1016/j.chemosphere.2019.02.148.
Huang, X., Zhou, T., Chen, X., Bai, J., Zhao, Y., 2022. Enhanced biodegradation of high-salinity and low-temperature crude-oil wastewater by immobilized crude-oil biodegrading microbiota. J. Ocean Univ. China 21 (1), 141–151. https://doi.org/10.1007/s11802-022-4907-4.
Ibrahim, H.M., 2018. Characterization of biosurfactants produced by novel strains of *Ochrobactrum anthropi* HM-1 and *Citrobacter freundii* HM-2 from used engine oil-contaminated soil. Egypt. J. Pet. 27 (1), 21–29. https://doi.org/10.1016/j.ejpe.2016.12.005.
Jabbar, N.M., Alardhi, S.M., Mohammed, A.K., Salih, I.K., Albayati, T.M., 2022. Challenges in the implementation of bioremediation processes in petroleum-contaminated soils: a review. Environ. Nanotechnol. Monit. Manag. 18, 100694. https://doi.org/10.1016/j.enmm.2022.100694.
Jain, D.K., Collins-Thompson, D.L., Lee, H., Trevors, J.T., 1991. A drop-collapsing test for screening surfactant-producing microorganisms. J. Microbiol. Methods 13 (4), 271–279. https://doi.org/10.1016/0167-7012(91)90064-w.
Jimtaisong, A., Sarakonsri, T., 2019. Chitosan intercalated bentonite as natural adsorbent matrix for water-soluble sappanwood dye. Int. J. Biol. Macromol. 129, 737–743. https://doi.org/10.1016/j.ijbiomac.2019.02.078.
Joseph, J.J., Sangeetha, D., Gomathi, T., 2016. Sunitinib loaded chitosan nanoparticles formulation and its evaluation. Int. J. Biol. Macromol. 82, 952–958. https://doi.org/10.1016/j.ijbiomac.2015.10.079.
Juhanson, J., Truu, J., Heinaru, E., Heinaru, A., 2009. Survival and catabolic performance of introduced *Pseudomonas* strains during phytoremediation and bioaugmentation field experiment. FEMS Microbiol. Ecol. 70 (3), 446–455. https://doi.org/10.1111/j.1574-6941.2009.00754.x.
Kamoun, E.A., Menzel, H., 2012. HES-HEMA nanocomposite polymer hydrogels: swelling behavior and characterization. J. Polym. Res. 19 (4), 9851. https://doi.org/10.1007/s10965-012-9851-3.
Kaur, P., Kaur, P., 2024. Synthesis and characterization of chitosan-bentonite biocomposite: parametric optimization and adsorption potential. J. Dispersion Sci. Technol. 1–12. https://doi.org/10.1080/01932691.2024.2325393.
Kaushal, J., Singh, G., Arya, S.K., 2018. Immobilization of catalase onto chitosan and chitosan–bentonite complex: a comparative study. Biotechnol. Rep. 18, e00258. https://doi.org/10.1016/j.btre.2018.e00258.
Kausar, A., Naeem, K., Hussain, T., Nazli, Z.I.H., Bhatti, H.N., Jubeen, F., Iqbal, M., 2019. Preparation and characterization of chitosan/clay composite for direct Rose FRN dye removal from aqueous media: comparison of linear and non-linear regression methods. J. Mater. Res. Technol. 8 (1), 1161–1174. https://doi.org/10.1016/j.jmrt.2018.07.020.
Kaya, F., Ozer, A., 2022. Selective sulfate sorption from boric acid factory process liquor: Chitosan-bentonite biocomposite film synthesis as sorbent. Miner. Eng. 187, 107777. https://doi.org/10.1016/j.mineng.2022.107777.
Khandelwal, A., Sugavanam, R., Ramakrishnan, B., Dutta, A., Varghese, E., Nain, L., Banerjee, T., Singh, N., 2022. Free and immobilized microbial culture–mediated crude oil degradation and microbial diversity changes through taxonomic and functional markers in a sandy loam soil. Front. Environ. Sci. 9, 794303. https://doi.org/10.3389/fenvs.2021.794303.
Khodabakhshloo, N., Biswas, B., Moore, F., Du, J., Naidu, R., 2021. Organically functionalized bentonite for the removal of perfluorooctane sulfonate, phenanthrene and copper mixtures from wastewater. Appl. Clay Sci. 200, 105883. https://doi.org/10.1016/j.clay.2020.105883.
Khondee, N., Tathong, S., Pinyakong, O., Müller, R., Soonglerdsongpha, S., Ruangchainikom, C., Luepromchai, E., 2015. Lipopeptide biosurfactant production by chitosan-immobilized *Bacillus sp.* GY19 and their recovery by foam fractionation. Biochem. Eng. J. 93, 47–54. https://doi.org/10.1016/j.bej.2014.09.001.
Kim, G.J., Kim, D., Lee, K.J., Kim, D., Chung, K.H., Choi, J.W., An, J.H., 2020. Effect of nano-montmorillonite on osteoblast differentiation, mineral density, and osteoclast differentiation in bone formation. Nanomaterials 10 (2), 230. https://doi.org/10.3390/nano10020230.
Knijnenburg, J.T., Kasemsiri, P., Amornrantanaworn, K., Suwanree, S., Iamamornphan, W., Chindaprasirt, P., Jetsrisuparb, K., 2021. Entrapment of nano-ZnO into alginate/polyvinyl alcohol beads with different crosslinking ions for fertilizer applications. Int. J. Biol. Macromol. 181, 349–356. https://doi.org/10.1016/j.ijbiomac.2021.03.138.
Kumar, A.P., Janardhan, A., Viswanath, B., Monika, K., Jung, J.Y., Narasimha, G., 2016. Evaluation of orange peel for biosurfactant production by Bacillus licheniformis and their ability to degrade naphthalene and crude oil. 3 Biotech 6, 1–10. https://doi.org/10.1007/s13205-015-0362-x.
Kuppan, N., Padman, M., Mahadeva, M., Srinivasan, S., Devarajan, R., 2024. A comprehensive review of sustainable bioremediation techniques: eco friendly solutions for waste and pollution management. Waste Manag. Bull. 2 (3), 154–171. https://doi.org/10.1016/j.wmb.2024.07.005.
Le Quoc, P., Solovieva, A.Y., Uspenskaya, M.V., Olekhnovich, R.O., Sitnikova, V.E., Strelnikova, I.E., Kunakova, A.M., 2021. High-porosity polymer composite for removing oil spills in cold regions. ACS Omega 6 (31), 20512–20521. https://doi.org/10.1021/acsomega.1c02517.
Lin, C., Gan, L., Chen, Z., Megharaj, M., Naidu, R., 2014. Biodegradation of naphthalene using a functional biomaterial based on immobilized *Bacillus fusiformis* (BFN). Biochem. Eng. J. 90, 1–7. https://doi.org/10.1016/j.bej.2014.05.003.
Liu, Y., Li, W., Qiao, Y., Yu, F., Wang, B., Xue, J., Zhou, Z., 2022. Study on the changes in immobilized petroleum–degrading bacteria beads in a continuous bioreactor related to physicochemical performance, degradation ability, and

microbial community. Int. J. Environ. Res. Publ. Health 19 (18), 11348. https://doi.org/10.3390/ijerph191811348.
Liu, Q., Wang, Y., Sun, S., Tang, F., Chen, H., Chen, S., Li, L., 2023. A novel chitosan-biochar immobilized microorganism strategy to enhance bioremediation of crude oil in soil. Chemosphere 313, 137367. https://doi.org/10.1016/j.chemosphere.2022.137367.
Luo, Q., Hou, D., Jiang, D., Chen, W., 2021. Bioremediation of marine oil spills by immobilized oil-degrading bacteria and nutrition emulsion. Biodegradation 32, 165–177. https://doi.org/10.1007/s10532-021-09930-5.
Mall, I.D., Srivastava, V.C., Kumar, G.V.A., Mishra, I.M., 2006. Characterization and utilization of mesoporous fertilizer plant waste carbon for adsorptive removal of dyes from aqueous solution. Colloids Surf. A Physicochem. Eng. Asp. 278 (1-3), 175–187. https://doi.org/10.1016/j.colsurfa.2005.12.017.
Majiya, H., Clegg, F., Sammon, C., 2023. Bentonite-Chitosan composites or beads for lead (Pb) adsorption: design, preparation, and characterization. Appl. Clay Sci. 246, 107180. https://doi.org/10.1016/j.clay.2023.107180.
Mehrotra, T., Dev, S., Banerjee, A., Chatterjee, A., Singh, R., Aggarwal, S., 2021. Use of immobilized bacteria for environmental bioremediation: a review. J. Environ. Chem. Eng. 9 (5), 105920. https://doi.org/10.1016/j.jece.2021.105920.
Mekonnen, B.A., Aragaw, T.A., Genet, M.B., 2024. Bioremediation of petroleum hydrocarbon contaminated soil: a review on principles, degradation mechanisms, and advancements. Front. Environ. Sci. 12, 1354422. https://doi.org/10.3389/fenvs.2024.1354422.
Mokhtar, A., Asli, B., Abdelkrim, S., Hachemaoui, M., Boukoussa, B., Sassi, M., Abboud, M., 2024. Polymer/Clay nanocomposites as advanced adsorbents for textile wastewater treatment. Minerals 14 (12), 1216. https://doi.org/10.3390/min14121216.
Morikawa, M., Hirata, Y., Imanaka, T., 2000. A study on the structure–function relationship of lipopeptide biosurfactants. BBA Mol. Cell Biol. Lipids. 1488 (3), 211–218. https://doi.org/10.1016/s1388-1981(00)00124-4.
Moussa, L.A., Azeiz, A.Z.A., Hassanien, S.E., 2017. Microbial biodegradation of crude petroleum oil as affected by salinity. Environ. Sci. 12 (1), 545–558. https://doi.org/10.21608/bces.2017.462896.
Muangchinda, C., Chamcheun, C., Sawatsing, R., Pinyakong, O., 2018. Diesel oil removal by Serratia sp. W4-01 immobilized in chitosan-activated carbon beads. Environ. Sci. Pollut. Res. 25, 26927–26938. https://doi.org/10.1007/s11356-018-2742-3.
Nayarisseri, A., Singh, P., Singh, S.K., 2019. Screening, isolation and characterization of biosurfactant-producing *Bacillus tequilensis* strain ANSKLAB04 from brackish river water. Int. J. Environ. Sci. Technol. 16 (11), 7103–7112. https://doi.org/10.1007/s13762-018-2089-9.
Olafadehan, O.A., Bello, V.E., Amoo, K.O., 2022. Production and characterization of composite nanoparticles derived from chitosan, CTAB and bentonite clay. Chem. Pap. 76 (8), 5063–5086. https://doi.org/10.1007/s11696-022-02228-7.
Pandey, L.M., 2019. Enhanced adsorption capacity of designed bentonite and alginate beads for the effective removal of methylene blue. Appl. Clay Sci. 169, 102–111. https://doi.org/10.1016/j.clay.2018.12.019.
Parach, A., Rezvani, A., Assadi, M.M., Akbari-Adergani, B., 2017. Biodegradation of heavy crude oil using Persian Gulf autochthonous bacterium. Int. J. Environ. Res. 11, 667–675. https://doi.org/10.1007/s41742-017-0059-6.
Partovinia, A., Rasekh, B., 2018. Review of the immobilized microbial cell systems for bioremediation of petroleum hydrocarbons polluted environments. Crit. Rev. Environ. Sci. Technol. 48 (1), 1–38. https://doi.org/10.1080/10643389.2018.1439652.
Patowary, K., Patowary, R., Kalita, M.C., Deka, S., 2017. Characterization of biosurfactant produced during degradation of hydrocarbons using crude oil as sole source of carbon. Front. Microbiol. 8, 279. https://doi.org/10.3389/fmicb.2017.00279.
Pete, A.J., Bharti, B., Benton, M.G., 2021. Nano-enhanced bioremediation for oil spills: a review. ACS EST Eng. 1 (6), 928–946. https://doi.org/10.1021/acsestengg.0c00217.
Pluangklang, C., Rangsriwatananon, K., 2021. Facile method by bentonite treated with heat and acid to enhance pesticide adsorption. Appl. Sci. 11 (11), 5147. https://doi.org/10.3390/app11115147.
Purnomo, A.S., Putra, S.R., Putro, H.S., Hamzah, A., Rohma, N.A., Rohmah, A.A., Rizqi, H.D., Tangahu, B.V., Warmadewanthi, I.D.A.A., Shimizu, K., 2023. The application of biosurfactant-producing bacteria immobilized in PVA/SA/bentonite bio-composite for hydrocarbon-contaminated soil bioremediation. RSC Adv. 13 (31), 21163–21170. https://doi.org/10.1039/d3ra02249h.
Queiroz, M.F., Teodosio Melo, K.R., Sabry, D.A., Sassaki, G.L., Rocha, H.A.O., 2015. Does the use of chitosan contribute to oxalate kidney stone formation? Mar. Drugs 13 (1), 141–158. https://doi.org/10.3390/md13010141.
Rissouli, L., Chabbi, M., Berradi, M., Eddaoukhi, A., Chaer, I., Znagui, F., Benicha, M., 2025. Chitosan-Bentonite composite adsorption of herbicide glyphosate from water solution. Environ. Monit. Assess. 197 (3), 1–19. https://doi.org/10.1007/s10661-025-13677-4.
Rostami, E., Norouzbeigi, R., Rahbar, A., 2018. Thermal and chemical modification of bentonite for adsorption of an anionic dye. Adv. Environ. Tech. 4 (1), 1–12. https://doi.org/10.22104/AET.2018.1844.1088.
Safdari, M.S., Kariminia, H.R., Ghobadi Nejad, Z., Fletcher, T.H., 2017. Study potential of indigenous *Pseudomonas aeruginosa* and *Bacillus subtilis* in bioremediation of diesel-contaminated water. Water Air Soil Pollut. 228, 1–7. https://doi.org/10.1007/s11270-016-3220-5.
Salsabila, N., Arifin, Y.F., Pratiwi, A.Y., 2024. Compaction parameters of a chitosan-bentonite-sand mixture. ICESDM. https://doi.org/10.4108/eai.2-11-2023.2348009, 2023.
Santoso, S.P., Kurniawan, A., Soetaredjo, F.E., Cheng, K.C., Putro, J.N., Ismadji, S., Ju, Y.H., 2019. Eco-friendly cellulose–bentonite porous composite hydrogels for adsorptive removal of azo dye and soilless culture. Cellulose 26, 3339–3358. https://doi.org/10.1007/s10570-019-02314-2.
Sayara, T., Sánchez, A., 2020. Bioremediation of PAH-contaminated soils: process enhancement through composting/compost. Appl. Sci. 10, 3684. https://doi.org/10.3390/app10113684.
Senol, Z.M., Ertap, H., Fernine, Y., El Messaoudi, N., 2024. Adsorptive removal of synthetic dye from its aqueous solution by using chitosan-bentonite composite: DFT and experimental studies. Polym. Bull. 81, 12795–12817. https://doi.org/10.1007/s00289-024-05323-9.
Sharma, D., Saharan, B.S., Chauhan, N., Procha, S., Lal, S., 2015. Isolation and functional characterization of novel biosurfactant produced by *Enterococcus faecium*. SpringerPlus 4, 1–14. https://doi.org/10.1186/2193-1801-4-4.
Sharma, I., 2020. Bioremediation techniques for polluted environment: concept, advantages, limitations, and prospects. In: Trace Metals in the Environment-New Approaches and Recent Advances. IntechOpen. https://doi.org/10.5772/intechopen.90453.
Siles, J.A., García-Sánchez, M., 2018. Microbial dynamics during the bioremediation of petroleum hydrocarbon-contaminated soils through Bio stimulation: an overview. In: Prasad, R., Aranda, E. (Eds.), Approaches in Bioremediation: the New Era of Environmental Microbiology and Nanobiotechnology. Springer Inc., Switzerland, pp. 115–134. https://doi.org/10.1007/978-3-030-02369-0_7.
Singh, R., Singh, S.K., Rathore, D., 2019. Analysis of biosurfactants produced by bacteria growing on textile sludge and their toxicity evaluation for environmental application. J. Dispersion Sci. Technol. 41, 510–522. https://doi.org/10.6084/m9.figshare.7945517.v2.
Singha, L.P., Pandey, P., 2021. Rhizosphere assisted bioengineering approaches for the mitigation of petroleum hydrocarbons contamination in soil. Crit. Rev. Biotechnol. 41 (5), 749–766. https://doi.org/10.1080/07388551.2021.1888066.
Sohail, R., Jamil, N., 2019. Isolation of biosurfactant producing bacteria from Potwar oil fields: effect of non-fossil fuel-based carbon sources. Green Process. Synth. 9 (1), 77–86. https://doi.org/10.1515/gps-2020-0009.
Soyuer, K., Bilen Ozyurek, S., 2024. An eco-friendly approach to biosurfactant production using low-cost wastes. J. Dispersion Sci. Technol. 45 (8), 1599–1612. https://doi.org/10.1080/01932691.2023.2225581.
Spini, G., Spina, F., Poli, A., Blieux, A.L., Regnier, T., Gramellini, C., Varese, G.C., Puglisi, E., 2018. Molecular and microbiological insights on the enrichment procedures for the isolation of petroleum degrading bacteria and fungi. Front. Microbiol. 9, 2543. https://doi.org/10.3389/fmicb.2018.02543.
Sun, W., Cao, W., Jiang, M., Saren, G., Liu, J., Cao, J., Ali, I., Yu, X., Peng, C., Naz, I., 2018. Isolation and characterization of biosurfactant-producing and diesel oil degrading *Pseudomonas* sp. CQ2 from Changqing oil field, China. RSC Adv. 8 (69), 39710–39720. https://doi.org/10.1039/C8RA07721E.
Tekere, M., Jacob-Lopes, E., Zepka, L.Q., 2019. Microbial bioremediation and different bioreactors designs applied. Biotechnol. Bioeng. 1-19. https://doi.org/10.5772/intechopen.83661.
Thio, C.W., Lim, W.H., Md Shah, U.K., Phang, L.Y., 2022. Palm kernel fatty acid distillate as substrate for rhamnolipids production using *Pseudomonas* sp. LM19. Green Chem. Lett. Rev. 15 (1), 83–92. https://doi.org/10.1080/17518253.2021.2023223.
Venosa, A.D., Zhu, X., 2003. Biodegradation of crude oil contaminating marine shorelines and freshwater wetlands. Spill Sci. Technol. Bull. 8 (2), 163–178. https://doi.org/10.1016/S1353-2561(03)00019-7.
Wahba, M.I., 2017. Chitosan-glutaraldehyde activated calcium pectinate beads as a covalent immobilization support. Biocatal. Agric. Biotechnol. 12, 266–274. https://doi.org/10.1016/j.bcab.2017.10.016.
Wang, K., Ma, H., Pu, S., Yan, C., Wang, M., Yu, J., Wang, X., Chu, W., Zinchenko, A., 2019. Hybrid porous magnetic bentonite-chitosan beads for selective removal of radioactive cesium in water. J. Hazard. Mater. 362, 160–169. https://doi.org/10.1016/j.jhazmat.2018.08.067.
Warr, L.N., Perdrial, J.N., Lett, M.C., Heinrich-Salmeron, A., Khodja, M., 2009. Clay mineral-enhanced bioremediation of marine oil pollution. Appl. Clay Sci. 46 (4), 337–345. https://doi.org/10.1016/j.clay.2009.09.012.
Wei, X., Peng, P., Meng, Y., Li, T., Fan, Z., Wang, Q., Chen, J., 2021. Degradation performance of petroleum-hydrocarbon-degrading bacteria and its application in remediation of oil contaminated soil. IOP Conf. Ser. Earth Environ. Sci. 766 (1), 012096. https://doi.org/10.1088/1755-1315/766/1/012096.
Xi, Y., Mallavarapu, M., Naidu, R., 2010. Preparation, characterization of surfactants modified clay minerals and nitrate adsorption. Appl. Clay Sci. 48 (1-2), 92–96. https://doi.org/10.1016/j.clay.2009.11.047.
Yang, Y., Xu, Y., Zhong, D., Qiao, Q., Zeng, H., 2024. Efficient removal of Cr (VI) by chitosan cross-linked bentonite loaded nano-zero-valent iron composite: performance and mechanism. J. Hazard Mater. 480, 136183. https://doi.org/10.1016/j.jhazmat.2024.136183.
Zhu, Z., Kou, H., Zhou, Y., Lan, X., Yu, M., Chen, H., 2023. Preparation of amphiphilic chitosan-loaded bentonite adsorbent and its performance in removing organic matter from coking wastewater. Polymers 15 (6), 1588. https://doi.org/10.3390/polym15061588.
Zommere, Z., Nikolajeva, V., 2017. Immobilization of bacterial association in alginate beads for bioremediation of oil-contaminated lands. Environ. Exp. Biol. 15 (2). https://doi.org/10.22364/eeb.15.09.